12-2009

A Study on Gas Penetration and Fingering Behavior in Injection Molding of Polymer and Powder Metal Feedstock

Edna I. Orozco
University of Texas-Pan American

A STUDY ON GAS PENETRATION AND FINGERING BEHAVIOR IN INJECTION MOLDING OF POLYMER AND POWDER METAL FEEDSTOCK

A Thesis

by

EDNA I. OROZCO

Submitted to the Graduate School of the
University of Texas-Pan American
In partial fulfillment of the requirements for the degree of

MASTER OF SCIENCE

December 2009

Major Subject: Manufacturing Engineering

A STUDY ON GAS PENETRATION AND FINGERING BEHAVIOR IN INJECTION MOLDING OF POLYMER AND POWDER METAL FEEDSTOCK

A Thesis

by

EDNA I. OROZCO

Dr. Kye-hwan Lee
Chair of Committee

Dr. Rajiv Nambiar
Committee Member

Dr. Seokyoung Ahn
Committee Member

Dr. Miguel Gonzalez
Committee Member

December 2009

ABSTRACT

Orozco, Edna I., A Study on Gas Penetration and Fingering Behavior in Injection Molding of Polymer and Powder Metal Feedstock. Master of Science (MS), December, 2009, 72 pp, 14 tables, 42 figures, references, 51 titles.

The effect of processing variables on the level of gas penetration in parts fabricated by gas-assisted injection molding from two different materials was compared. The materials used were polypropylene and stainless steel powder metal/thermoplastic feedstock. Software simulation and physical experiments were conducted. Taguchi analysis was used to reduce the number of experiment trials and to find the optimum processing conditions. Four different variables were changed using nine different combinations. The processing variables are the pressure, the delay time before gas is injected, the temperature of the material injected, and the amount of the material injected. The results showed that the most critical variable in the experiment is shot size followed by gas pressure, delay time and material.

DEDICATION

First of all I am grateful to God for those He sent me to guide me on my way, for those He gave me as a family of my own to fill my heart to overflowing with the greatest love I've ever known, a wonderful family who supports me and gives me the strength in my life. I would like to dedicate this thesis to my husband and family. Thanks for their unconditional love.

ACKNOWLEDGEMENTS

First of all I thank God for each precious blessing including the times filled with challenges. I would like to express my gratitude to all those who gave me the possibility to complete this thesis. I want to thank the faculty of the department of Manufacturing Engineering for facilitating the equipment, tools and knowledge for my research work and thesis.

I have furthermore to thank Dr. Nambiar and Dr. Kevin Lee for whose help, stimulating suggestions and encouragement helped me in all the time of research and writing of this thesis. In addition I want to thank my committee members for their assistance; I express my most sincere gratitude to Dr. Gonzalez and Dr. Seokyoung Ahn for their help, support, interest and valuable hints. Also I want to thank Leticia Ocanas, Rene Maldonado and Hector Arteaga for their help and advice throughout these years at school at the Manufacturing Processes Lab.

Especially, I would like to give my special thanks to my husband Rene Leonhardt, whose patient love enabled me to complete this work looked closely at the final version of the thesis for English style and grammar, correcting both and offering suggestions for improvement. Lesly Orozco, Hiram Orozco, and my parents whose love and encouragement helped me to finish one more chapter in my life, and I know they will continue supporting me in my life.

TABLE OF CONTENTS

Page

LIST OF TABLES

Page

LIST OF FIGURES

Page

CHAPTER I

INTRODUCTION

1.1 Injection Molding Process

Injection molding (IM) process one of the most common processes used to fabricate small to mid-size plastic parts. The injection molding process is used in mass production of thermoplastic components because of its ability to make complex parts with high tolerances and good details on the surface of parts. In this process, raw material in the form of solid pellets is fed into the hopper that is located above the rear end of the barrel of the injection molding machine. When the resin makes contact with the heated barrel it starts melting. The resin is pushed towards the mold by a screw that rotates and generates friction between the material and the barrel. The screw heats and mixes the resin so that it is completely molten when it arrives at the front end of the barrel. A fixed quantity of the molten resin is then injected through a sprue into the mold. Once the resin is in the mold the material is allowed to cool down and solidify to the desired dimensions and shape [1]. The cycle of this process starts with the closing of the mold, this means that both plates are pushed in contact to each other with a high force. The next step in the cycle is the injection of the molten material which flows through the sprue and gets to the gate where material is directed to the cavity of the mold. Once the part is full it is necessary to hold the pressure in the mold until the part solidifies, this is known as packing [2]. If proper

packing pressure is not applied, defects like sink marks and voids may form. It is then necessary to let the material cool down, and this time depends on the mold material and the design of the parts being made.

When the resin starts to solidify in the mold, the next shot is prepared by the screw rotation in the barrel. Material enters the barrel through the hopper, which is cooled to avoid melting of the pellets before they reach the barrel. The barrel has three different zones; in the first zone the screw pushes the pellets and softens them, in the second zone the screw melts the material through shearing and the last zone contains the melt at the desired temperature ready to be injected in the mold [3]. The screw plays an important role in this process; when it rotates, it heats the material with friction and enough pressure to melt the material, and by going backwards it loads the amount of material necessary for the shot of the next part. Once cooling cycle time is over and part is solid in the mold, the mold opens slowly, releasing the vacuum caused in the injection molding process [4]. Finally the cycle is completed when the mold opens and the part is ejected by means of the ejector pins.

1.1.1 Injection Molding Machine

Fig 1-1 shows how the injection molding machine is divided in 3 main areas in which each of them have different and specific purposes [5].

- Injection Unit: The main purpose of this unit it is to heat and inject the material into the mold. It includes a hoper, barrel, nozzle, heating bands, and screw. The material is poured into the hoper in the shape of pellets; the bottom of the hoper is open allowing the barrel to be fed with material. The barrel has a mechanism that

consists in a screw that primarily heats and injects the molten plastic into the mold.

- Mold Assembly: Molten parts get the shape of the mold. A mold is a cavity where molten material is forced to fill the empty space. Molds are divided in 2 parts in order to be able to extract the final product, one side of the mold is fixed and the other side is the ejection part or moving side. Molds need a distribution channel that consists of a sprue, runners, and gates that allow the material to flow to the cavity. Ejector pins are part of the moving side of the mold; they push the part out of the mold.
- Clamping Unit: This part of machine is used for different functions. It allows opening and closing of the mold, it holds the mold while the material is being injected, and finally ejects the part when it is ready.

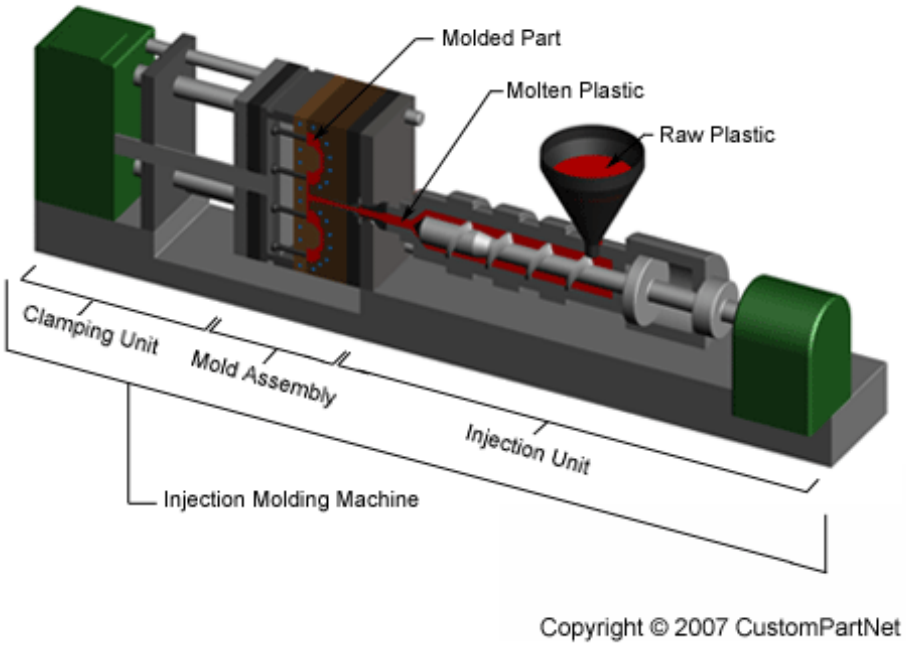

Figure 1- 1: Injection Molding Machine [47]

1.1.2 Advantages and Disadvantages of Injection Molding Process

Some of the advantages of injection molding are the ability to produce a high amount of parts in a short period of time with high tolerances with low cost of labor, and no need of machining of the parts. Also the waste of material is low because the parts made are very precise with the mold. However the major disadvantage is that the mold and the equipment are very expensive. It is not convenient to produce in small quantities, because of the cost of the mold [6].

1.2 Rapid Prototyping Technologies

Rapid Prototyping (RP) is a set of innovative technologies that has a lot of applications, and these include the making of a working model or a prototype with different purposes such as testing design, features, functionality, and performance, among others. One of the major benefits of RP is the reduction of the risk mass producing a part along with the production costs [7]. There are several different technologies available in the market, but all fabricate parts with the same procedure listed below:

- Model of the component on a CAD system
- CAD model is converted into a computerized format that approximates its surfaces (STL file format)
- Slicing of the model into layers

The major technologies are categorized in the Table 1.

Table 1-1: Rapid Prototyping Technologies

Prototyping technologies	Base materials
Selective laser sintering (SLS)	Thermoplastics, metals powders
Fused deposition modeling (FDM)	Thermoplastics, eutectic metals.
Stereolithography (SLA)	Photopolymer
Laminated object manufacturing (LOM)	Paper
Electron beam melting (EBM)	Titanium alloys
3D printing (3DP)	Various materials

1.2.1 Stereolithography (SLA)

This is the oldest and most dominant of the RP processes. Part fabrication is accomplished as a series of layers that are solidified on the surface of a vat of liquid epoxy resin as shown in Figure 1-2; each layer is added onto the previous layer as the part sinks with the platform into the vat to gradually build the 3-D geometry. Each layer is 0.076 mm to 0.50 mm (0.003 in to 0.020 in.) thick. Thinner layers provide better resolution and more complex shapes; but processing time is longer. Polymerization of the liquid monomers occurs on exposure to UV light of the laser scanning beam [8].

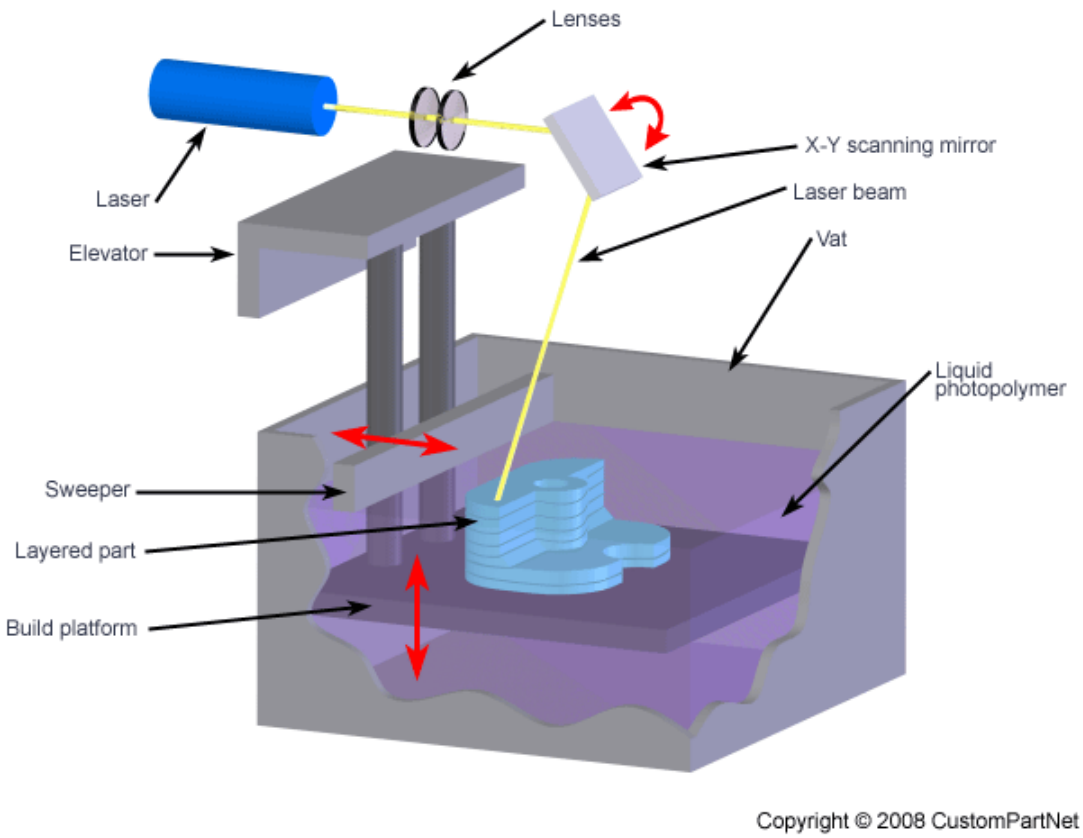

Figure 1- 2: Stereolithography: Beginning of the process, initial layer is added to the platform; several layers have been added to the part [48]

Materials Used for this technology

- ACCURA 60 (near transparent Poly-Carbonate like resin)
- ACCURA 25 (opaque white Polypropylene like resin)
- SL 7820 (opaque near black ABS-like resin)
- SOMOS NanoTool (high temp ceramic filled resin)

The epoxy resin is a thermosetting polymer and so is just strong enough at the melting temperature of many common thermosetting polymers so that it can be used to fabricate mold materials [9]. This process becomes competitive when the number of parts needed does not justify the high cost and time required to fabricate a metal mold.

Functional parts are needed for design verification testing, field trials, customer evaluation, and production planning. By eliminating multiple steps, the creation of the injection mold directly by a rapid prototyping (RP) process holds the best promise of reducing the time and cost needed to mold low-volume quantities of parts. Stereolithography technology with the integration of injection molding is still missing is the fundamental understanding of how the modifications to the mold material and RP manufacturing process impact both the mold design and the injection molding process. In recent years manufacturers have found an increased need to shorten product development cycles in order to achieve a quicker time to market new products. The use of stereolithography parts as injection molding tools, offers many advantages over traditional tool making approaches. One of them is the time require to convert a computer aided design (CAD) file to the final tool is dramatically reduced as may be the cost in creating the tool. The stereolithography process may be used to create an injection molding tool in which plastic material will be injected although the main problem encountered using stereolithography is that the tool breaks due to many reasons. Stereolithography tools have material properties such as tensile strength, Young's modulus and shear strength which are considerably lower than those for metals such aluminum or steel. The problem gets worst by the increase in temperature of the mold

and further deterioration in mechanical properties when hot plastic is injected[41]. As a result of these failures, molders have abandoned the use of this technology after some unsuccessful attempts.

1.2.2 Selective Laser Sintering (SLS)

A moving laser beam sinters powders in areas corresponding to the CAD geometry model one layer at a time to build the solid part. Once each layer is completed, a new layer of loose powders is spread across the surface. Layer by layer, the powders are gradually bonded by the laser beam into a solid mass that forms the 3-D part geometry as shown in Figure 1-3. In areas not sintered, the powders are loose and can be poured out of completed part [10]. Unlike stereolithography, SLS prototyping techniques allow prototypes to be made with material properties closer to that of injection molded pieces and it also has the capability to make metal prototype parts where metallic powder is used in the laser sintering process. Another advantage is that there is typically very little processing required after the selective laser sintering is completed [43].

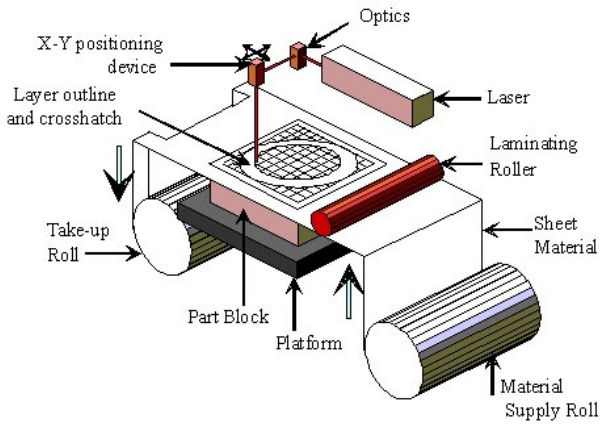

Figure 1- 3: SLS Process [49]

Some of the comparisons of stereolithography and selective laser sintering are that stereolithography process is limited to photosensitive resins which are typically brittle. The SLS process can utilize polymer powders that, when sintered, approximate thermoplastics quite well. The surface of an SLS part is powdery, like the base material whose particles are fused together without complete melting. The smoother surface of a stereolithography part typically wins over SLS when an appearance model is desired. Stereolithography is more accurate immediately after completion of the model [46].

1.3 Powder Injection Molding

In the powder injection molding process, the feed stock is a mixture of metal powder and binder which is injected under pressure into a mold using a conventional injection molding machine. The powder injection molding process combines metal, ceramic or carbide powders with a binder in order to inject this material into a mold using conventional plastic injection molding machines. The binder, known as feedstock, is removed; the problem with this method is that a large amount of shrinkage occurs during sintering [11]. There are also some other limitations in this process like thick sections due to cooling, packing, sink marks on the surface. All these defects become a challenge because the purpose of injection molding is to get the best part produced at the lowest possible cost and time. This process has been limited to small parts due to the high cost of the feed stock and poor cavity filling. Recently, researchers have made efforts to overcome these limitations using Gas-assisted Injection Molding (GAIM). Materials such as metals, alloys, ceramics, cermets and composites have been produced by PIM.

1.4 Gas Assisted Injection Molding (GAIM)

GAIM uses pressurized nitrogen to push the injected feed stocks in to the mold; this provides better surface finish, shorter cycle time and also reduces the weight of the parts. However, the effects of processing variables over the process have not fully understood. GAIM was an innovation of Friederich [12]. The advantages of it are to provide a better surface finish, shorter cycle time and also reduce the weight of the parts. Some other advantages are; stress free molding and sink free molding [13].

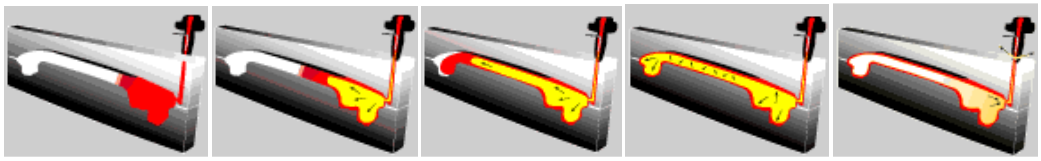

Figure 1- 4: (1) "short shot" of thermoplastic, (2)gas shut off valve is used, (3) nitrogen is injected into the center of the hot resin, (4) all of the surfaces receive an equal pressure creating an even "pack out" of the part, (5) nitrogen gas is vented [50]

Figure 1-4 shows the GAIM process which takes the pressurized gas and injects it into the melt penetrating the cross-sectioned gas channels. This process is able to complete partially or volumetric fillings of a specific cavity with polymer melt, as in injection molding.

After material has been injected next phase is the injection of nitrogen, this gas is used because of its availability, cost, and inertness. After this phase, pressure is released either by releasing the gas or by recycling it. As soon as ambient pressure is reached, the molded part can be ejected [14].

Once melting occurs and gas is being injected, the material being melt solidifies forming walls in the outer part of the material, and it forms a solid layer of resin. This layer tends to grow depending on the material used, during the delay of the gas injection. At the time gas injection happens, the compressed nitrogen runs through the plastic core and pushes some of the molten material. At the time when this happens, is when the plastic is in the stage of packing, but with GAIM process this stage prevents void formation, because the gas performs the packing, and the voids are designed to reduce cycle time and part weight. Nitrogen gas is used in the GAIM because its viscosity is lower than the polymer melt. For this reason, the pressure drop over the flow length of the gas bubble is much lower than over the flow length of a molded part. The pressure drop in the holding and packing phase influences the shrinkage across the part and the ability to pack a part. Shrinkage differences promote buildup of internal molded-in stresses and subsequently influence the warpage of a part significantly. The gas-assist process reduces internal stresses and warping and thus improves part quality. It provides a higher and more evenly distributed packing pressure across the part, resulting in better overall part flatness. [15]

There are several gas assisted injection technologies available and the main difference between them is where the compressed gas is injected. Gas can be injected through the nozzle or through runners [41].

CHAPTER II

REVIEW OF LITERATURE

2.1 Gas-Assisted Injection Molding Process

The injection molding process has been changing a lot throughout the time gaining more importance in the industry. This process has changed from the production of simple parts like combs, to the production of parts for the medical, automotive and aerospace industry [16]. By 1872, John and Isaiah Hyatt patented the injection molding machine. Even though it was not a very advanced machine it was able to accomplish the basic purpose. It contained a basic plunger to inject the plastic into a mold through a heated cylinder [17]. Injection molding is a process that produces parts in a repetitive way by melting the material, and then injecting it to a cavity insert or mold, followed by the solidification of the part, and later the ejection of it. In order to produce effectively there are some steps that have to be considered for this process which are; material selected for the parts, design of the part, design of the mold, and the processing conditions of the material used [18]. One of the disadvantages of this process that has become a challenge is to improve the quality of the parts produced while keeping the cost of producing them low. There is a new technology that attracts more and more injection molders and it is called Gas Assisted Injection Molding (GAIM). GAIM is the application of gas, generally nitrogen, to the conventional injection molding process for hollow parts. As a result, this technology offers several benefits: an excellent surface appearance; gas injection parts

have a higher stiffness-to-weight ratio than solid parts with the same dimensions; dimensional stability is improved and post mold warpage and sink marks are reduced due to more uniform wall thickness and lower residual stress thought the part; less cycle time needed and less part weight, stress free, sink free, and increased part design freedom [19]. Since this process is new, most of the information about it comes from trial an error through the years, and there is a learning curve associated with processing and optimization [20].

2.2 Control, Design, and CAE of GAIM Process

One of the critical characteristics for GAIM is to be able to control this process and this is one of the reasons that make this field one of the most rapidly growing in the area of control and process development. Molders and industry have raised concerns over controlling the injection of the gas. Even though gas injection equipment gives the opportunity to make adjustments to the process, it is still necessary to establish an optimum process window that will provide control and repeatability of the process to mold consistent and acceptable parts [19]. Due to the interest in controlling the gas in the process many companies offer a gas injection molding unit that it mainly controls the pressure or the volume of gas in the process [21]. In order to develop this process it was necessary to understand it, starting from the design area up to the experimental trials nowadays one of the advantages is the opportunity to simulate this process and to study the processing conditions and parameters involved in the gas-assisted process with Moldflow Pty Ltd, of Australia [22]. The only design and production analysis tools available for GAIM were experienced based rules, and due to the growing of the market

demand, Moldflow developed a software package that predicts material and gas flow within the mold. This software provides the ability to predict material/gas fill pattern, anticipation of gas blow, and establish processing conditions [23].

It has become possible to predict the mold filling process with melt and gas using the finite element method. Research by Moritzer and Potente [24] showed how an optimization method can be employed to systematically convert a molding for the gas injection molding process. GAIM is a process that involves complex correlation between the molded part geometry and the associated process parameters and it has been approached by trial and error, with the valves employed being empirical ones. They developed a method based on a systematic design procedure employed for conventional injection moldings with 6 phases offering a standardized concept for the layout of GAIM components.

- Phase 1, Planning: Design job is selected and the specific development assignment established.
- Phase 2, Concept: Compilation of requirements for the product to be created.
- Phase 3, Design: Establish conventional layout process for the product which means material, shape, and dimensions of the product are defined.
- Phase 4, Optimization: Molded parts are optimized from the production engineering view. This part is possible with the help of FE simulations.
- Phase 5, Elaboration: Compilation of the molded part drawing from which the product is to be manufactured. This drawing contains all kinds of details of the geometric dimensions and precise details of the surface and material to be used for the part.

- Phase 6: Molding is sampled at the optimum operating point and adjustments are made to the mold where necessary.

As a result of this study is possible to show that the optimized approach represents a considerably more efficient method of producing GAIM. Once there is a plan to follow for this process it is important to take in consideration other conditions and parameters. In 1935, Fairbrother [25] conducted the first experiments investigating the flow phenomena using a viscous Newtonian solution. He found that *m (fractional coverage or fraction of liquid deposited on the walls of the tube after bubble penetration,* is a function of the capillary number, C_a, for capillary numbers up to 0.009. The fractional coverage, *m*, is defined for the tube-shaped geometries as:

$$m = A_p/At_t = 1 - (r_b/R)\text{^}2 \qquad \text{Eq. 2.1}$$

$$C_a = \eta U_b / \Gamma \qquad \text{Eq. 2.2}$$

A_p= polymer cross-sectional area

A_t= tube cross-sectional area

r_b= radius of gas bubble

U_b= product of bubble velocity

η = Viscosity of the fluid

Γ = fluid surface tension

Taylor [26] investigated this problem further in 1961 and ran experiments that extended to capillary numbers of two. Cox [27] found that the fractional coverage

reached a value of m= 0.60 for capillary numbers greater than ten for viscous Newtonian Fluids.

Polinski and Stokes [28] conducted similar experiments using silicone liquid. Koelling et al [29] conducted gas-assisted injection molding experiments using a spiral tube mold and three common injection molding grade compounds: polystyrene, polyvinyl, chloride, and polycarbonate. By measuring the wall thickness along the flow path of the gas bubble, the residual time, gas bubble velocity, and material properties were found to be responsible for changes in fractional wall coating thickness as much as 20%. Polymer melts which begin to shear thin at low shear rates are more sensitive to changes in gas pressure and gas pistol speed, while those polymers that have significant upper Newtonian regions are relatively insensitive to these changes.

To take advantage of the GAIM process the study on gas-assisted in recent years are focused on the construction of the development of computer-aided-engineering (CAE) technology, Chen Yew-Renn and Chen Tay-Yuan [30] introduced a method of combining the CAE technology with the design guidelines to sizing the gas channels of a gas- assisted injection mold. One of the key factors that determine the successful application of this new process is the design of gas channels which guide the gas flow to the desired locations. The design of gas channels requires to be laid out in the early stage of part design. If the layout of gas channels and their corresponding dimensions and shapes in cross sections are not properly designed, catastrophe often happened in the molded parts; therefore the gas channel design is one of the critical points to that affect the flow of gas in the GAIM process. For the gas channel with larger diameter,

it not only can provide bigger available volume of polymer melt to fulfill the empty region, but also can reduce the flow resistance during filling since the gas channel acts as a flow leader. In the paper by Chen et al [31] an approach is provided so that the channel diameters are chosen by the criterion of mass balance based on the presuming values of ratio of deposited thickness to the channel radius. Although the value of ratio of deposited thickness to the channel radius is affected by some other factors. It is reasonable to assume 0.2 and 0.5 as the lower and the upper limits. The lower limit is for a strong shear-thinning, and the upper one is for a smaller shear-thinning and strong cooling effect. For gas penetrating in channel without permeation, the available melt volume per length the deposited thickness and the channel diameter has a simple relation shown in the formula bellow.

$$V_a=\Pi D^2 (1-\delta)^2 / 4 \qquad \text{Eq. 3}$$

V_a = available melt volume per length

D= channel diameter

$\delta=\frac{b}{(D/2)}$ where b= deposited melt thickness

To further confirm the design and find possible weakness such as air traps, flow simulation software is introduced into the design procedure. Finally the optimum one is picked up according to the result and related engineering judgment. The experiment showed the following results:

- Distribution of the coating melt thickness is relatively uniform behind the gas front during the primary penetration period, and it decreases with increasing gas pressure.
- Skin melt thickness increases when the melt temperature decreases.
- Close to the gas front, the coating melt thickness shows 2 types of characteristics, one is that at low injection gas pressures and longer delay times, the coating thickness at the gas front first decreases and then increases, creating a melt-thinning region of a gas swell shape. At high pressures and short delay times, the skin melt thickness around the gas front increases as a result of melt shrinkage during the secondary penetration stage.

2.3 Stereolithography in GAIM Process

When designing a part with this type of process it is necessary to design functional parts that are needed for verification testing, field trials, costumer evaluation, and production planning. Creating a mold for this process with rapid prototyping technology will time and cost needed to mold low-volume quantities of parts. Unfortunately current simulation packages for conventional injection molding are no longer applicable to this new type of injection molds. Huamin Zhou and Dequn Li [32] integrated an approach to accomplish a numerical simulation of injection molding into rapid-prototyped molds, and developed a corresponding simulation system. They compared the experimental results with the simulation verification Figure 2-2, which showed that their method handles RP fabricated with Stereolithography (SLA) molds.

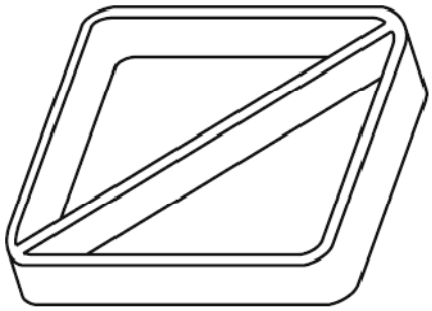

Figure 2- 1: Experimental Cavity Model [32]

The cavity used for their experiment has the dimensions of 36×36×6 mm as shown in Figure 2-1. The thickness dimensions of the thin walls and rib are both 1.5 mm. The cavity surface is subjected to the melt pressure, the surfaces of the mold connected to the worktable are fixed in space, and other external surfaces are assumed to be stress free.

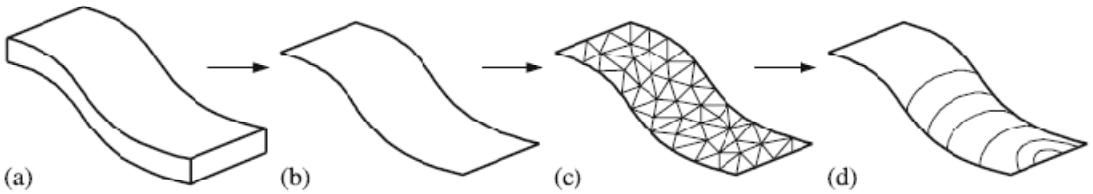

Figure 2- 2: Schematic procedure of the simulation with middle-plane model. (a) The 3-D surface model (b) the middle-plane model (c) the meshed middle-plane model (d) the display of the simulation result [32]

The results of the developed model give a closer outcome to the experimental results. It was found that the effect of temperature is more dominant than the pressure; therefore an improvement in the thermal conductivity of the photopolymer can improve the part quality significantly.

Nambiar et al [9] investigated how to extend the life of plastic injection molds made by Stereolithography through the use of gas-assist technology by comparing conventional injection molding with gas-assisted injection molding. They evaluated the life of the SLA mold that included 2 mm core pins Figure 2-3 shows the cavity geometry and the location of the pins in the cavity insert. It was found that the evenly applied gas pressure helped increase the core pin life by 115 percent. There is a three-fold increase in ejection force when using GAIM. Observations indicate the majority of the pin failures for both methods do indeed occur during part ejection rather than during melt injection.

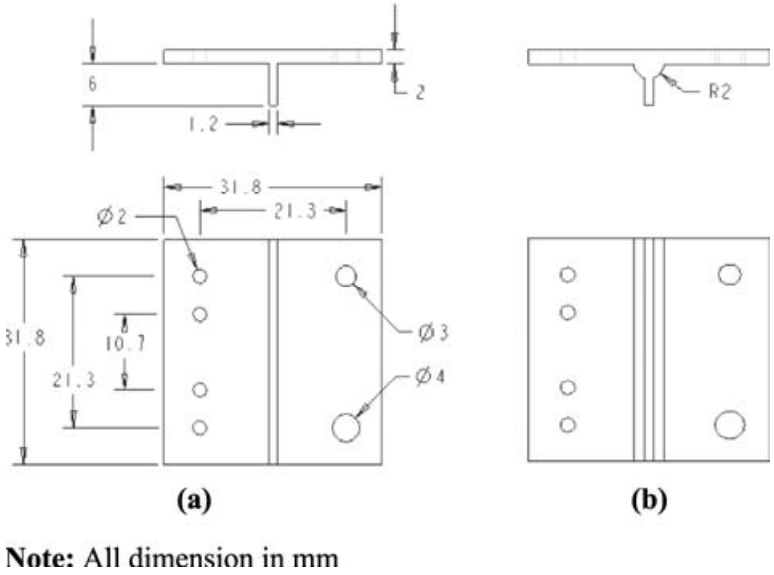

Figure 2- 3: Part design for (a) conventional injection and (a) for Gas Assisted Injection Molding [9]

2.4 Powder Injection Molding and GAIM Processes

Gas-assisted injection molding is no longer only for plastic materials, the powder injection molding (PIM) process is an efficient method for the high volume production of shaped components from powders. PIM is a derivative of polymer injection molding and

uses much of the same technology, along with batch sintering processes used in powder metallurgy and ceramic processing.

Hemrick et al [33] studied the behavior of powder injection molded (PIM) part and the Stereolithography epoxy mold surrounding it after cooling. It was found that the release behavior of injection molded parts using SLA-epoxy molds is an important factor for consideration in the use of rapid tooling for powder injection molding. In the case of SLA-epoxy molds, relatively high injection temperatures and subsequent large shrinkage during cooling leads to the formation of a surface layer on the mold. Lower injection temperatures, however, lead to parts with good surface finish but which adhere to the mold surfaces making it difficult to remove the cooled part from the mold.

Ahn et al. [34] research is focus on the powder injection molding area, their studies analyzed the filling, packing and cooling stages of powder injection molding (PIM) with the geometry shown in Figure 2-4. The integrated CAE analysis of filling, packing and cooling was examined with 316L stainless steel PIM. The conclusion from their study is that the characteristics between the filling and cooling analysis should be considered for the integrated CAE analysis of PIM parts. The reason for the consideration is because the cavity wall temperature is as a boundary condition for the energy equation and this value is determined from the cooling analysis.

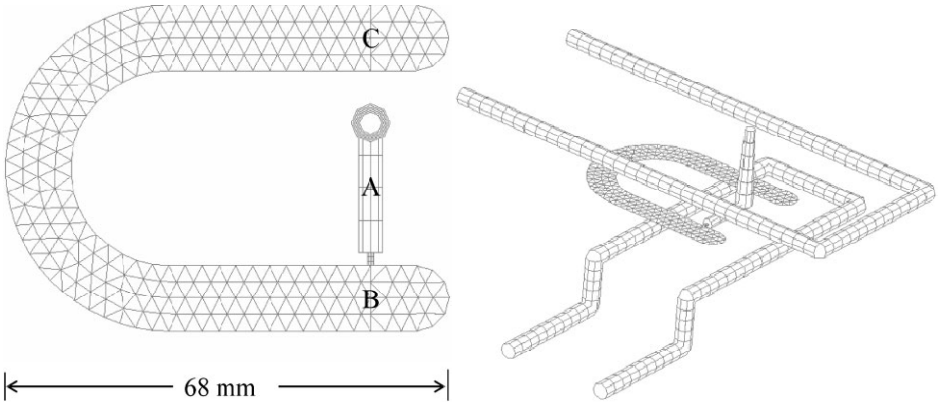

Figure 2- 4: Cooling channel layout and part geometry for U-shaped [34]

A comparison between simulated and experimental pressures in a U-shaped mold Figure 2-5 showed that the consideration of slip behavior and the coupled analysis between the filling, packing and cooling stages provided more accurate results. The increase in accuracy can be attributed to the fact that viscosity and slip layer of powder–binder mixture highly depend on temperature.

Figure 2- 5: Simulation Analysis showing average mold cavity wall temperature distributions [34]

Similar studies were performed by Berginc et al [35] they investigated the influence of the main injection molding parameters and the sintering conditions. The results showed that optimal injection molding parameters are necessary in order to avoid high shrinkage deviations after sintering Figure 2-6. The shrinkage shows that the injection molding parameters have an important role when narrow tolerances need to be achieved. On the basis of the Taguchi approach it was established that the most influential parameters are the temperature of the mould and the material, the holding pressure and the cycle time. The mold temperature has the largest effect, the higher the mould temperature, the smaller the shrinkage of the specimen and the smaller the dimensional deviations.

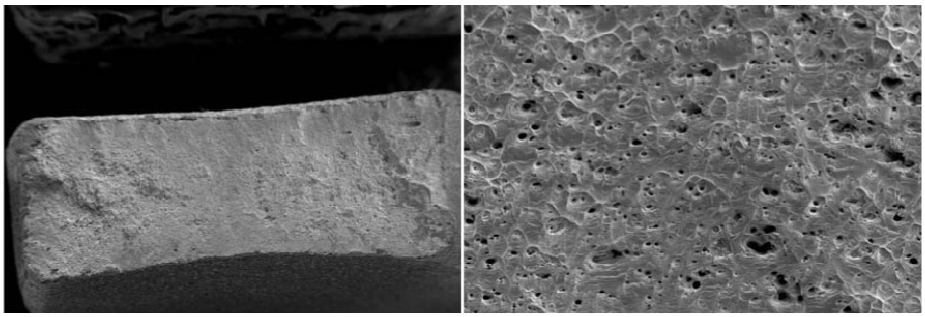

Figure 2- 6: Fractured surface of sintered specimen under optimal sintering and molding conditions [35]

In addition to controlled parameters, uncontrolled ones are also important, and they proved to be crucial in the performed experiments. An inappropriate choice of material for the supports, the incorrect disintegration of the binder, the atmosphere, a too high heating rate and sintering temperature, impurities, and a too slow cooling rate can drastically deteriorate the mechanical properties and dimensions of sintered parts.

Khakbiz et al. [36] work is about the rheological behavior of powder injection molding feedstock comprising of 316L stainless steel and 3 wt-%TiC powders by using a capillary rheometer. The results show that TiC addition plays an important role in rheological parameters, also the flow activation energy decreases with the introduction of TiC particles. Regarding the injection molding view the optimum PIM condition for the SS/TiC composite powder containing a wax based binder system was found at 55% solid volume fraction and 70uC. At this condition, the viscosity of feedstock is low enough to fulfill the requirements of a medium pressure, injection molding process.

CHAPTER III

METHODOLOGY

The primary objective of this experiment is to observe both the gas filling and the fingering behavior in gas assisted injection molding. De Hoyos 2009 studied the behavior of GAIM with a cylindrical geometry as shown in Figure 3-2; however, the geometry was entirely a gas channel, and this does not allow the study of the fingering effect. A cavity with a nominal wall and rib was designed to allow both gas penetration in the gas channel, and fingering of the gas into the nominal wall region. This chapter explains how the experiment was conducted by explaining procedures, materials and equipment used, and the simulation results obtained.

3.1 Design of Part and Cavity Insert:

3.1.1Part Design

First step on the experiment is the design of the part able to satisfy the primary purpose of this research. The design of the part will be different from De Hoyos' 2009 experiment which consisted in a circular geometry that allows the *gas penetration length.* The design of this experiment consisted basically in a rectangular geometry with nominal walls and a gas channel in the center as shown in Figure 3-1.

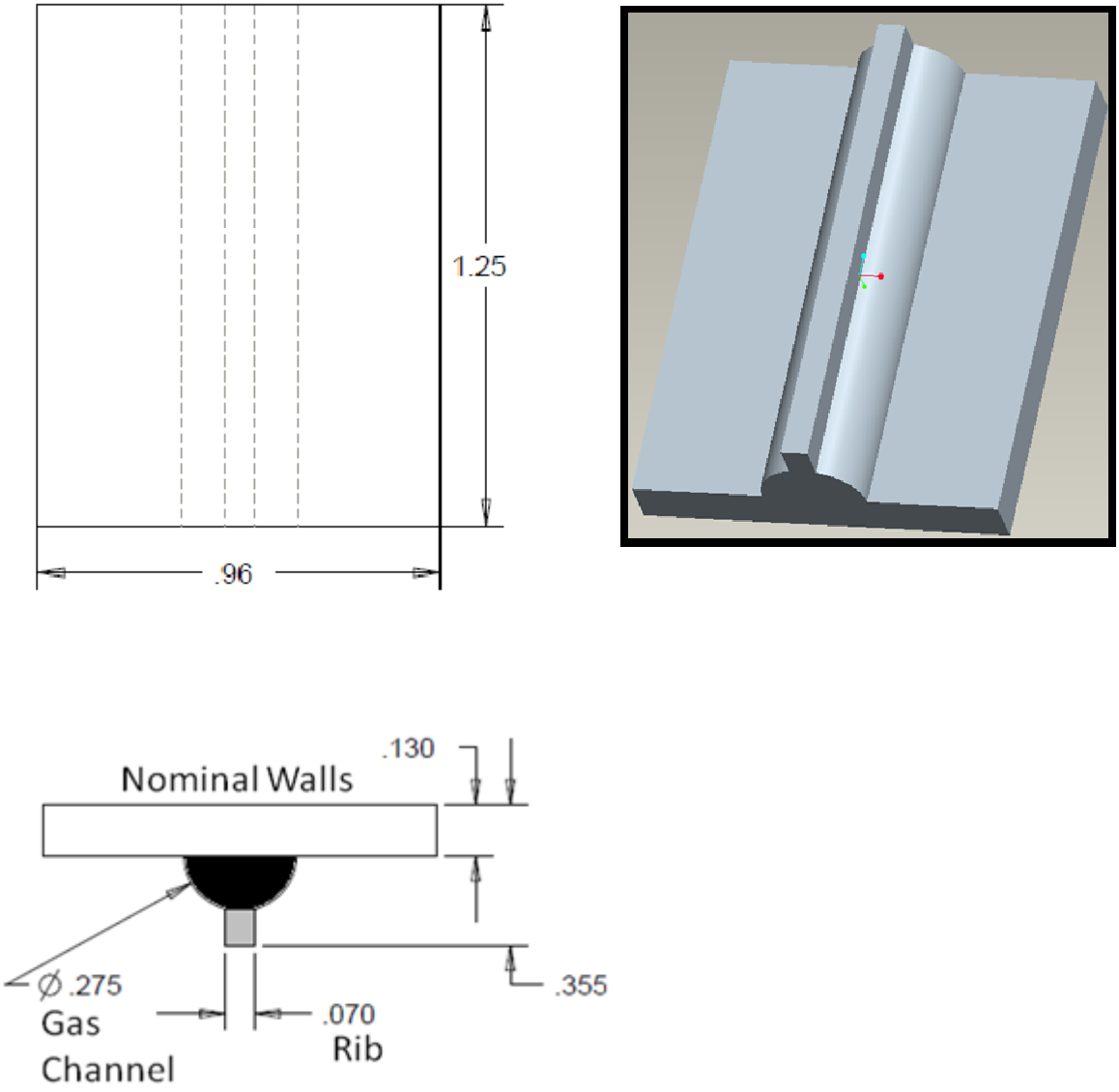

Figure 3- 1: Drawing of Part Design, Rectangular Geometry with Gas Channel, Nominal Walls and Rib

The geometry consists of a horizontal nominal wall and a vertical rib with a gas channel in the center which permits nitrogen to penetrate deep into the cavity. The plastic is first inserted into the part through the sprue, and then gas enters through the gate flowing through the gas channel giving the desired shape to the injected part as shown in Figure 3-2. This geometry of the cavity insert allowed the measurement of the gas flow, and to observe the fingering effect outside the gas channel.

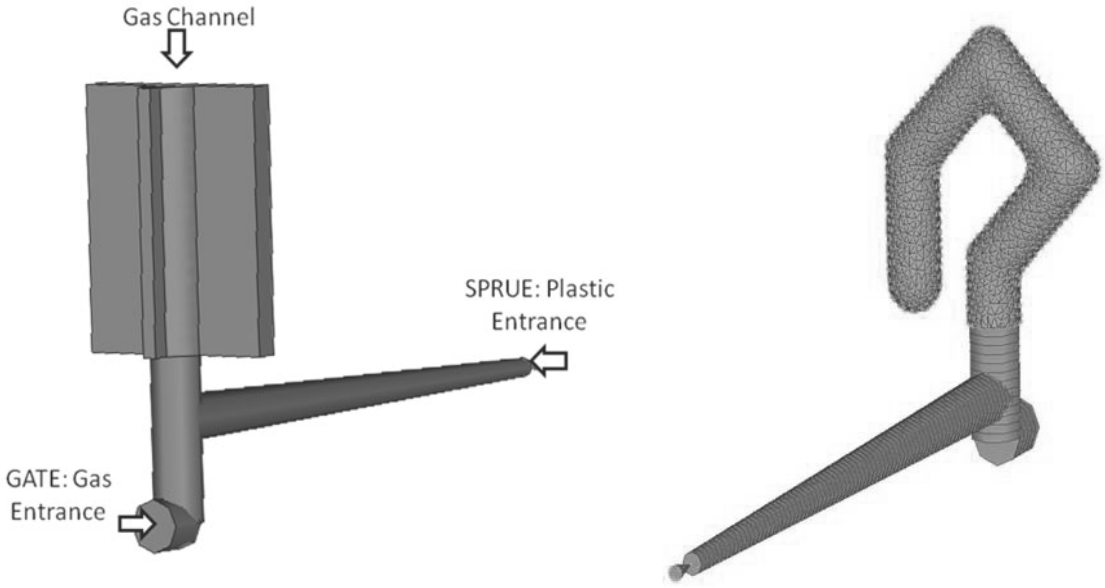

(1) (2)

Figure 3- 2 Rectangular Geometry Design used to compare the flow of gas through the gas channel next, (2) Cylindrical Geometry Used in De Hoyos' 2009 Research which follows a gas channel shape

3.1.2 Cavity Insert Design

The cavity insert with four ejector pin holes shown in Figure 3-3 was designed in PRO/Engineer. A thermocouple was located near the center, between the gas channel and

one of the ejector pins. One pressure transducer was located at the end of each of the two ejector pins that lie on the gas channel.

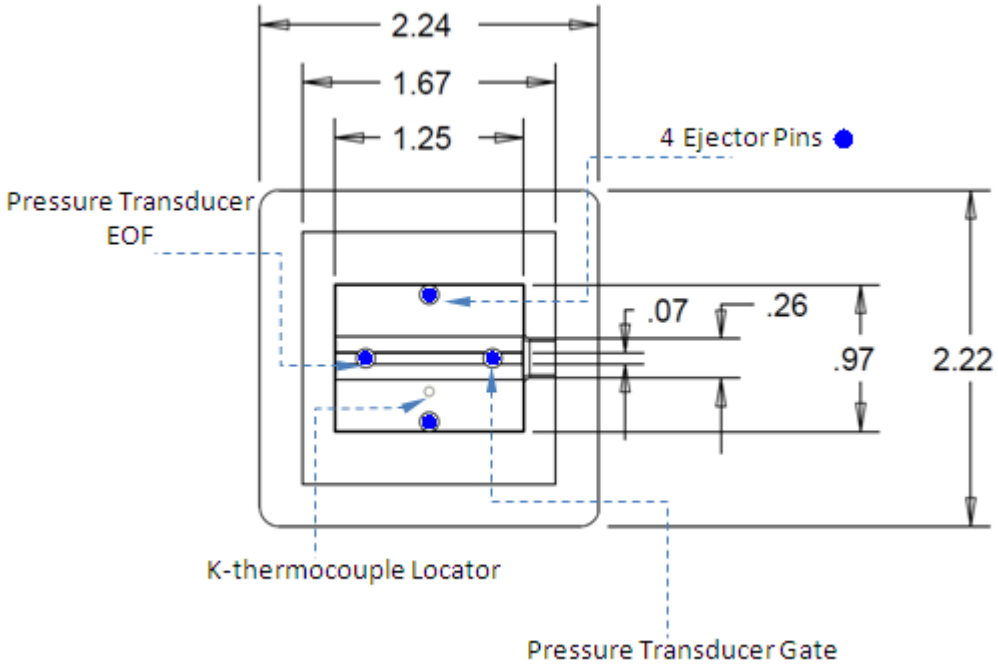

Figure 3- 3: Location of Instrument Readers on Stereolithography Cavity Insert

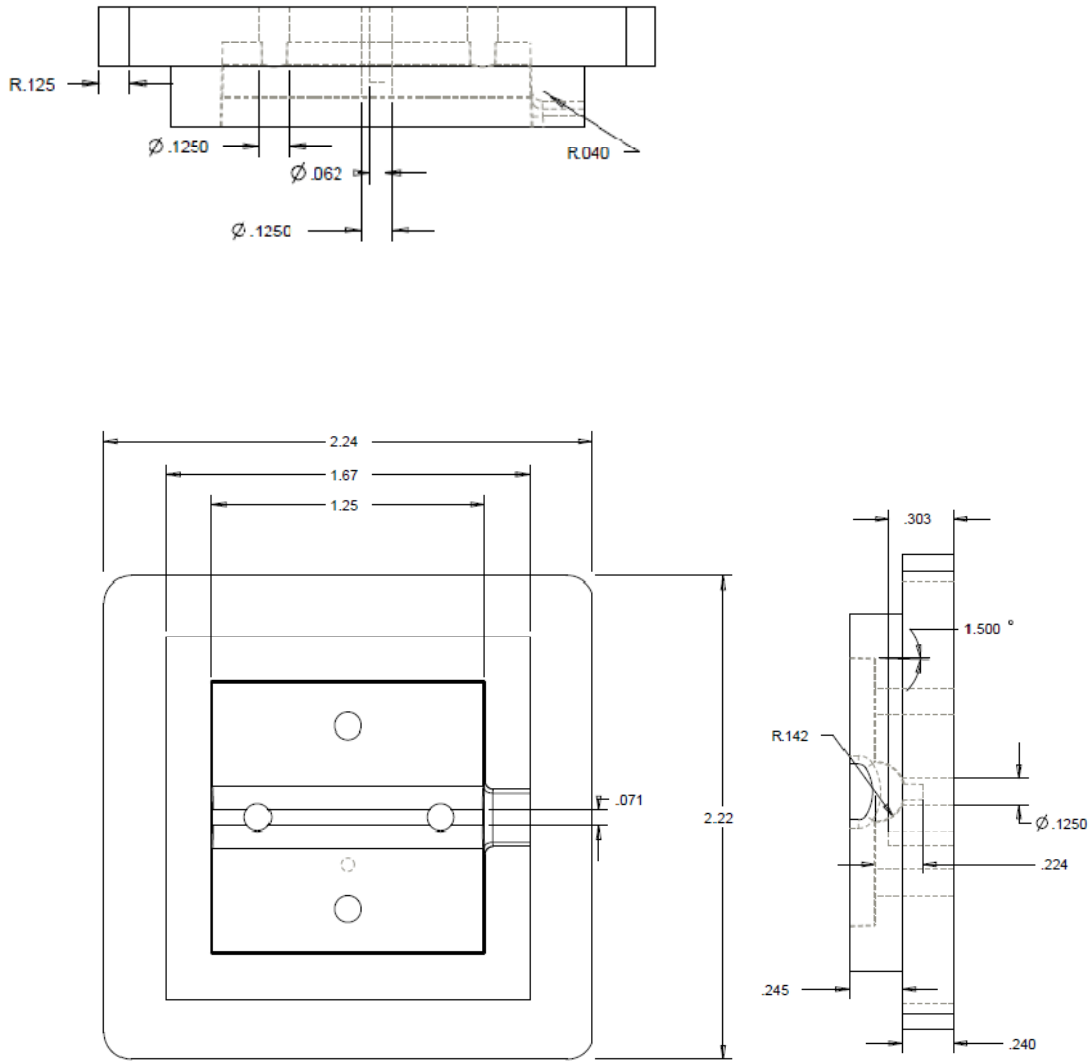

Figure 3- 4: Drawing of Cavity Insert with Dimensions in Inches

The cavity was fabricated using Stereolithography in a VIPER™ Pro SLA system shown in Figure 3-5. The geometry was converted to an STL file and then processed using 3D Lightyear ™.

Figure 3- 5 : VIPER™ Pro SLA system used for the manufacture of the cavity inserts for both materials in the experiment [51]

The specifications of this machine are shown bellow in Table 3-1.

Table 3-1: 3D systems VIPER™ PRO specifications

PARAMETER	MEASUREMENT
LASER	
Type	Solid-state frequency tripled Nd:YVO4
Wavelength	354.7 nm
Power - typical (at head) new	2000 mW
Power (warranty) - at vat @ 5000 hrs.	1000 mW
SOFTWARE	
Software	3DManage™ and 3DPrint™
Operating system	Windows XP Professional (Service Pack 2)
Input data file format	.stl, .slc
Network type and protocol	Ethernet, IEEE 802.3 using TCP/IP and NFS
AMBIENT TEMPERATURE	
Temperature range	20 - 26 °C (68 - 79 °F)
Maximum change rate	1 °C/hour (1.8 °F/hour)
Relative humidity	10 - 50 % non-condensing

The fabricated cavity insert is shown Figure 3-6. The model was sliced in layers of 0.101mm thickness. After the cavity insert was fabricated, the ejector pin holes were reamed. The cavity was then mounted on the aluminum mold base and place in the MUD Quick Mold Change Base and mounted in the BOY 30M injection molding machine.

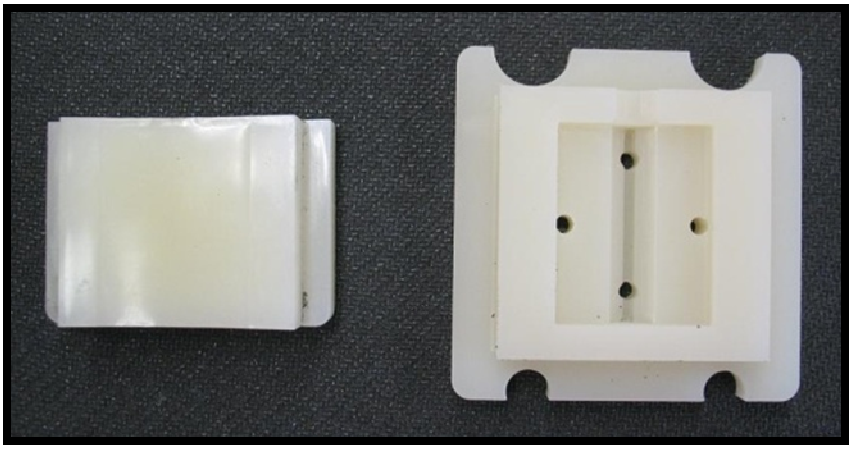

Figure 3- 6: Cavity Insert made out of Accura25 Material with Stereolythography Technology

The resin used for the cavity inserts was Accura® 25. Technical data of this material is shown in Table 3-2.

Table 3-2: Technical data sheet for Accura® 25

Liquid Material		
MEASUREMENT	CONDITION	VALUE:
Appearance		White
Liquid Density	@ 25 °C (77 °F)	1.14 g/cm3
Solid Density	@ 25 °C (77 °F)	1.19 g/cm3
Viscosity	@ 30 °C (86 °F)	250 cps
Penetration Depth (Dp)		4.2 mils
Critical Exposure (Ec)		10.5 mJ/cm2
Tested Build Styles		FAST™, EXACT™, Exact HR
Post-Cured Material		
MEASUREMENT	CONDITION	VALUE:
Tensile Strength	ASTM D 638	38 MPa (5,450 - 5,570 PSI)
Tensile Modulus	ASTM D 638	1,590 - 1,660 MPa (230 - 240 KSI)
Elongation at Break (%)	ASTM D 638	13 - 20 %
Flexural Strength	ASTM D 790	55 - 58 MPa (7,960 - 8,410 PSI)
Flexural Modulus	ASTM D 790	1,380 - 1,660 MPa (200 - 240 KSI)
Glass Transition (Tg)	DMA, E”	60 °C (140 °F)

3.2 Processing Materials and Equipment

3.2.1 Materials

This experiment was carried out with two different materials. For the powder metal feedstock, SUS316L from CetaTech (Sacheon, South Korea) was used. This material contains 59 per cent 316 stainless steel powder metal with a polypropylene based binder. For comparison, FHR Polypropylene (PP) 13T10Acs279 by Flint Hills Resources was used. This polypropylene was used in the experiment because of its optical semi-transparency which it makes easy to obverse the gas penetration behavior. Further, the binder in the SUS316L powder metal stainless steel feed stock, was also polypropylene.

3.2.2 Equipment

Injection molding is performed with a BOY30 that is shown in Figure 3-6.

Figure 3- 7: Injection Molding Machine BOY 30M

Table 3-3 shows the processing conditions for the experiment for both materials.

Table 3-3: Fixed processing conditions for Polypropylene and SUS316L

Injection Pressure	Hold Pressure	Back Pressure	Clamping Force	Screw Speed
6.89 MPa	6.89 MPa	0.517 MPa	11.03 MPa	50 rpm

A Chromega®-Alomega® (K) TT-J-30-SLE wire thermocouple type from Omega Engineering, Inc. was glued at the back of the cavity 2 mm bellow the top surface. A National Instruments data acquisition board was used to read the real time mold temperature changes from the thermocouple. The temperature measurements taken with this equipment helped to ensure that cavity insert was working at the desired temperature. The gas for this experiment was generated by a Gain Technologies (GT-N2GA) nitrogen generator shown in Figure 3-7. This equipment is has a membrane filter and separates the nitrogen from compressed air up to a purity of 99.5% at 2500 psi. A gas control system from HEA International was used. This gas control system uses a Tescom microcontroller ER3000, with a 26-1021 series regulator.

Figure 3- 8: GAIN Technology Nitrogen Generator

The cavity pressure was measure with two Kistler 6183AE pressure transducers. The first one was positioned close to the gate, and the other close to the end of fill. The ejection force was measured at the gate with a Kistler 9204BQ01 indirect cavity pressure transducer.

3.3 Design of Experiments:

This experiment has the target of maximizing the *gas penetration depth* and minimizing the *fingering width.* It was necessary to plan and conduct a number of trials in order to obtain sufficient and significant data. Taguchi analysis was used for the design of this

experiment. This method was used because it is based on an orthogonal array that reduces the variance (noise) in the results of the experiment by having the optimum settings of control parameters [29, 30]. Orthogonal Arrays provide a minimum number of experiments and Taguchi's Signal-to-Noise ratios (S/N), which is log functions of desired output; for this reason the Taguchi Method was used in this experiment in order to determine the best levels of control factors, which are those that maximize the Signal-to-Noise ratios for *gas penetration length* and minimize the signal to noise ratio for *fingering width*. Table 3-4 shows the distribution of the factors with their respective array number that was performed in the experiment.

Table 3-4: Taguchi Experimental L9

Trial #	Melt Temp.	Shot Size	Gas Pressure	Gas Delay
1	Low	Low	Low	Low
2	Low	Medium	Medium	Medium
3	Low	High	High	High
4	Medium	Low	Medium	High
5	Medium	Medium	High	Low
6	Medium	High	Low	Medium
7	High	Low	High	Medium
8	High	Medium	Low	High
9	High	High	Medium	Low

In Taguchi analysis there are variables that are under control, and variables that are not under control in other words, Control Factors and Noise Factors, respectively. The factors under control throughout the experiment are *melt temperature*, *shot size*, *gas pressure* and

gas delay. The experiment needs to be perform in a randomize order in order to reduce noise to the results. Other researchers have used this method to maximize the gas penetration in gas assisted injection molding. Liu and Chang [41] made and experimental matrix design based on the Taguchi method to investigate the processing factors that affect the length of gas penetration. Also Taguchi design provided a very efficient and effective way to study the effects of processing parameters in research by Zhu et al. [45]. De Hoyos' experiment [18] with the purpose of finding maximum gas permeation in with gas assisted injection molding is based on Taguchi analysis.

In order to obtain the maximum *gas penetration length* in the Taguchi design analysis, the larger is better formula was used;

$$SN = -10 \times \log 10\left(\left|\frac{\sum \frac{1}{y^2}}{N}\right|\right)$$

and to obtain the minimum *fingering width*, the smaller is better formula was used.

$$SN = -10 \times \log 10\left(\left|\frac{\sum y^2}{N}\right|\right)$$

3.4 Processing Conditions for Injection Molding Experiments

Since Accura25, which is an epoxy material, has very low thermal conductivity and allows poor heat dissipation through the surrounding mold base, mold cavity temperature control during the injection stage is mainly governed by the heat input from the molten material that is injected into the cavity. An average wait of 2 minutes was allowed between shots, and this allowed the mold cavity temperature to return 30° C before each

cycle. This was done to maintain the cavity temperature below its T_g of 60ºC to prevent damage to the cavity insert.

The processing parameters under investigation are: *melt temperature, shot size, gas pressure,* and *gas delay* time, as these are known from previous research to be the most significant parameters for GAIM [5, 13, 15, 17]. It was necessary to determine a processing window for both materials by determining the lower and upper limit condition for the factors. These values were found by trial and error, taking in consideration the material properties for polypropylene and stainless steel powder, which means, it was not possible to inject the material above a certain temperature because the material degrades or below a certain pressure because the material would not be able to fill the cavity insert. These values were provided by the companies that supply these materials. Table 3-5 shows the values used in the experiment for polypropylene, and Table 3-6 show the values used in the experiment for SUSL316.

The processing windows identify the range in which the settings may vary. This experiment was randomized with the purpose of reducing noise in the results of gas penetration and fingering effect. In order to obtain five good samples, five samples were first discarded because it takes about five shots before the process becomes stable. The molded parts were cut and gas penetration depth was measured with Vernier calipers. Average gas penetration depth and fingering area were obtained by measuring 5 molded samples in each experimental trial specified by the Taguchi orthogonal array similar to research by Han et al [13].

Table 3-5: Initial Settings for Polypropylene

Trial #	Matrix #	Melt T. (°C)	Shot Size (mm)	Gas P. (Mpa)	Gas D. (secs)
5	1	193	6.8	5.17	0.0
9	2	193	7.0	5.51	0.5
6	3	193	7.2	5.86	1.0
7	4	204	6.8	5.51	1.0
2	5	204	7.0	5.86	0.0
3	6	204	7.2	5.17	0.5
4	7	215	6.8	5.86	0.5
1	8	215	7.0	5.17	1.0
8	9	215	7.2	5.51	0.0

Table 3-6: Initial Settings for SUS316L

Trial #	Matrix #	Melt T. (°C)	Shot Size (mm)	Gas P. (Mpa)	Gas D. (secs)
5	1	150	9.5	5.51	0.0
9	2	150	9.7	5.86	0.2
6	3	150	9.9	6.20	0.4
7	4	155	9.5	5.86	0.4
2	5	155	9.7	6.20	0.0
3	6	155	9.9	5.51	0.2
4	7	160	9.5	6.20	0.2
1	8	160	9.7	5.51	0.4
8	9	160	9.9	5.86	0.0

3.5 Simulation

One of the advantages of injection molding process is that complicated parts can be analyzed by simulation before production, thus avoiding high costs and time delays. Moldflow Plastics Insight software was used to simulate the process. This software was used to predict flow of the molten material in the cavity and also the *gas penetration length* in both the *polypropylene* and the *SUS316L feed stock.*

In order to run the simulation it is necessary to mesh the part, the mesh provides the basis for the analysis, where molding properties are calculated at every node. The part was meshed into 28142 elements as shown in Figure 3-7:

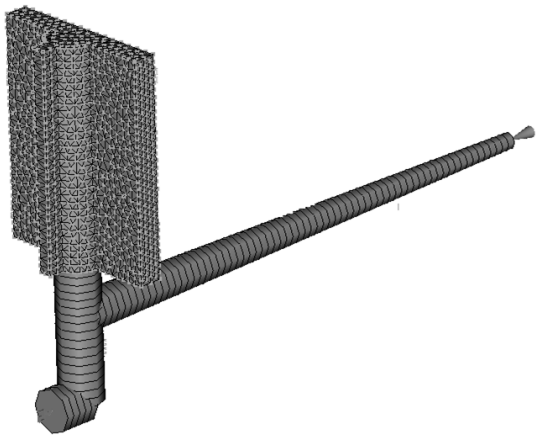

Figure 3- 9: Meshed Part for Simulation Analysis

The software was able to predict the *gas penetration length* and the *fingerin*g *width*. These results were compared with the experimental results.

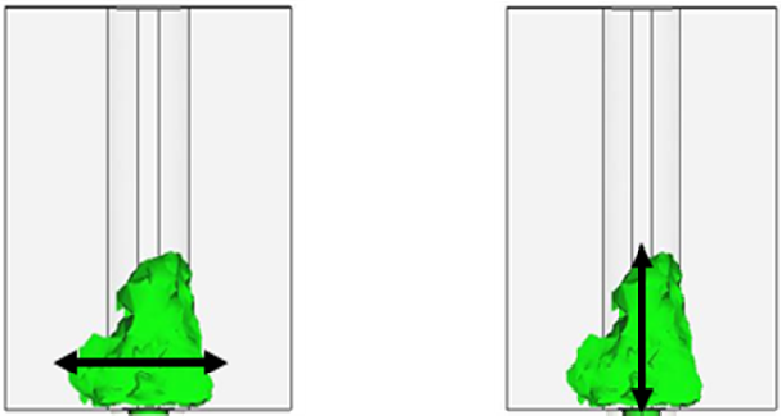

Maximum Fingering (mm) (1)

Maximum Gas Penetration (mm) (2)

Figure 3- 10: Shaded Area Demonstrates the Gas Penetration in Simulation Shots. (1) Fingering Width is measured horizontally; (2) Gas Penetration is measured vertically.

The results of the simulation display how the gas pattern does not flow only through the gas channel as shown in Figure 3-8, it actually flows towards the nominal walls of the cavity, in this case this result would be consider undesirable flow of gas, this is called fingering effect. In this experiment *fingering with* will be taken in consideration when it exceeds 6.604 mm which is the width of the gas channel. Severe gas fingering can results in significant reduction in part stiffness, impact strength and reliability of the final molded parts [45].

The properties of polypropylene were already contained in the MPI software, and the properties for SUS216L were imported into the software. The mold cavity material properties were also imported into the MPI software.

The full Taguchi analyses were carried out with 3 levels and 4 variables exactly as was done in the experiment. Thus, there were 9 simulations for each material and gas penetration length and fingering were measured in each case.

After calculating the S/N ratio from the measured data, analysis was conducted to get the optimal process settings. Once optimal settings were found, the verification simulation was run to obtain the optimized gas penetration and the fingering effect.

3.6 Experimental Procedures

In the experiment, the first 5 parts made in each trial were discarded as scrap. This step is necessary because by making these parts we allow the machine to stabilize the pressure, temperature and shot size. There is a waiting time of 2 minutes between each part to return the mold to room temperature. The next 5 molded parts were kept and labeled with their respective trial number. This experiment was randomized in order to decrease noise in the results.

Gas penetration and fingering effect of the parts were measured with Vernier calipers. The average of the measurements from the 5 good samples was used to get the average gas penetration depth and fingering effect.

The SUS316L molded parts had to be cut and open in order to measure them. In order to obtain optimal process settings it was necessary to make an S/N ratio analysis. After analyzing information results, simulations, and main effect plots we got the optimal process settings. A final verification experiment was conducted by testing the optimal settings to maximize the gas penetration depth and minimize the fingering effect.

CHAPTER IV

RESULTS AND DISCUSSION

In this chapter, the experimental and simulation results for *polypropylene* are presented first. This is followed by the results for the powder metal *SUS316L feedstock*. The final section investigates the wall thickness of the powder metal parts.

4.1 Results for Polypropylene

The results of the experiment are presented first. This is followed by the results of the computer simulation and a comparison of the results from two approaches.

4.1.1Experiment with Polypropylene

Figure 4-1 shows the main effect plot for *gas penetration length* and Figure 4-2 shows the main effect plot for *fingering width* in the *polypropylene* experiment. The Figures indicate that *shot size* has the highest effect on both. The *shot size* has a very strong negative effect on the *gas penetration length*; similar results were observed in the experiment by De Hoyos' [18], where the *shot size* was found to be the most critical variable for *gas penetration length*. As can be seen in Figure 4-2, the *shot size* also has a negative effect on the *fingering width*.

The effect of *melt temperature* is to increase both the *gas penetration length* and the *fingering width*. The *gas pressure* also appears to have a similar positive effect on both the *gas penetration length* and the *fingering width*. The *gas delay time* does not seem to have any significant effect on *gas penetration length*; however, the *fingering width* is higher at the mid-range of the *gas delay time*.

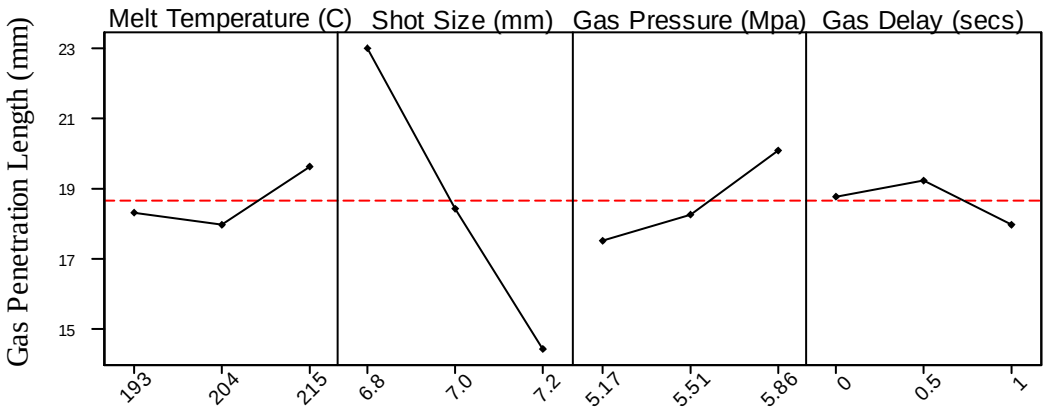

Figure 4-1: Main Effect Plot for Gas Penetration Length in Polypropylene Experiment

Each of the variables used in this experiment give a combination of values that will finally provide the maximum *gas penetration length*, although *melt temperature* and *gas pressure*, they appear to follow a similar pattern. For both variables it is necessary to select the high level value in order to maximize the target of this experiment. For *shot size* the plot shows a very high difference between the three levels used and the one that gives a maximum *gas penetration length* is the low level. The medium level value has to be selected for g*as delay* variable according to the main effect plot.

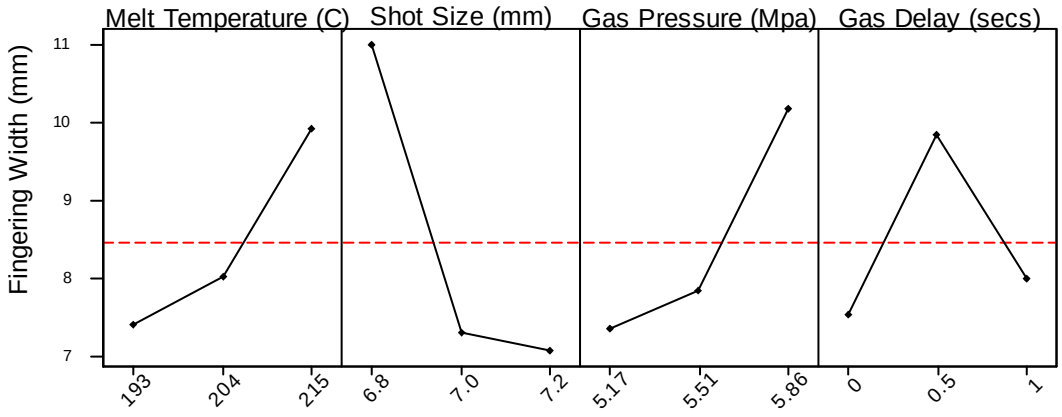

Figure 4-2: Main Effect Plot for Fingering Width in Polypropylene Experiment

In order to minimize the fingering width it would be necessary to select those variables with the lowest point in the main effect plot. M*elt temperature* and *gas pressure* variables seem to have the same pattern in which low level needs to be used. For *gas delay* variable the Figure 4-2 shows that the low level should be selected. A high level of s*hot size* is found to be the dominant for the reduction of *fingering width*.

The average of five samples for the *gas penetration length* and the *fingering width* are shown for each row in the Taguchi orthogonal L9 array for *polypropylene* in Figure 4-3. The parts made with the settings specified by array row numbers 1, 4 and 7 in the Taguchi orthogonal array are the ones with low *shot size* and these have higher *gas penetration length*. Array number 7 has the highest *gas penetration length* with the highest *fingering width*; this is not desirable and this indicates the low *shot size* is not always desirable for geometry with thin walls supported by ribs.

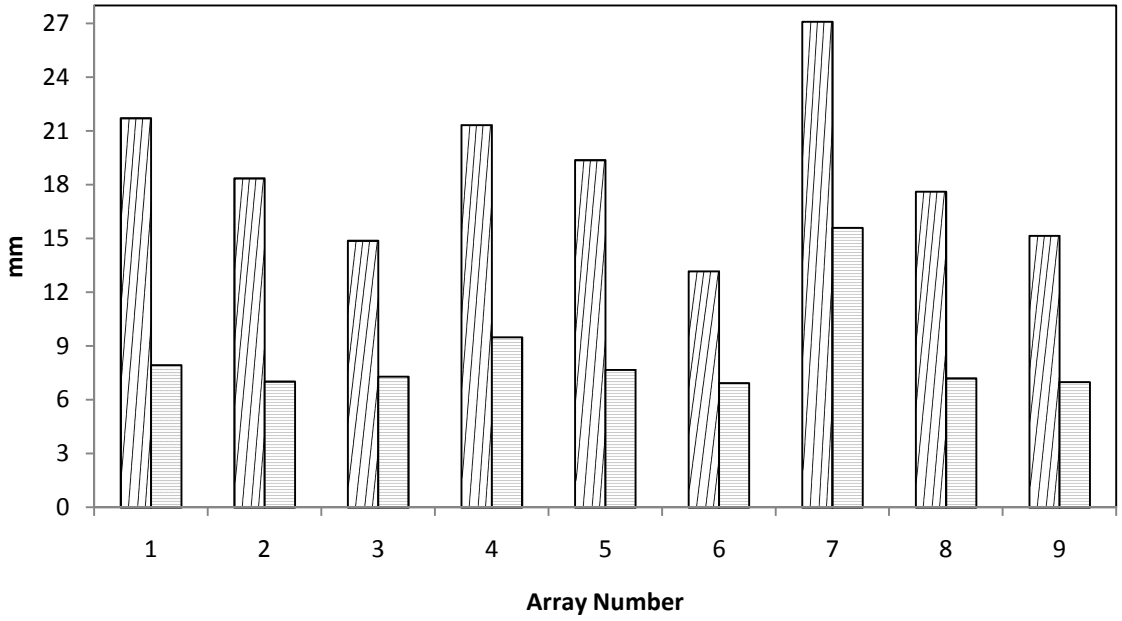

Figure 4-3: Gas Penetration Length and Fingering Width in Polypropylene Experiment

Larger the better signal to noise ratio (S/N ratio) for *gas penetration length* is calculated as well as smaller the better signal to noise ratio for *fingering width.* Table 4-1 shows the rank and percent significance of each of the processing variables based on the calculated S/N ratios.

Table 4-1: Significance of the Processing Variables for Experiment with Polypropylene

	Melt Temperature	Shot Size	Gas Pressure	Gas Delay
Gas Penetration Length	3 19.2%	1 41.0%	2 24.4%	4 15.17%
Fingering Width	2 20.2%	1 59.3%	4 8.1%	3 12.3%

The *shot size* had the highest significance among all the variables for both *gas penetration length*, with a portion of 41.0% of the effect, and also for *fingering width*, with 59.3% of the effect. For *gas penetration length*, the *gas pressure* was ranked second with 24.4% of the effect, followed by *melt temperature* with 19.2% of the effect, and the *gas delay time* was the least important parameter with 15.2% of the effect. In the case of the *fingering width* the main variable affecting is shot size with almost 60% of significance, followed by the next three variables *melt temperature, gas delay time* and *gas pressure* were almost equally significant.

The results of this experiment are similar to Parvaez et al. [40] in which they explore different variables that affect the gas distribution and the *fingering width* formation with different geometries, their results agree with the conclusion that *shot size* is a dominant factor that affects the gas penetration and fingering formation for parts fabricated by GAIM. Liu and Chang [41] identified other variables that affect these two factors. Their study, based on experimental results, concluded that melt temperature, gas injection delay time and gas hold time were the key processing parameters in full-shot gas assisted injection molded parts.

Since the target in this experiment is to maximize the *gas penetration length* and minimize the *fingering width*, it is necessary to obtain the optimal processing settings for each of the four processing variables. This is possible by analyzing a main effect plot for *gas penetration*. The optimum settings based on the main effect plot are shown in Table 4-2.

Table 4-2: Optimum Settings for Gas Penetration and Fingering Width

Variables	Maximum Gas Penetration Length	Minimum Fingering Width
Melt Temperature	High	Low
Shot Size	Low	High
Gas Pressure	High	Low
Gas Delay	Medium	Low

The gas penetration and the fingering can be observed in Figure 4-4. Due to the translucency of the *polypropylene* it is easy to recognize the *gas penetration length* and the *fingering width* effect in each of the parts made. Part 6.1, which was produced with the settings specified by the 6th row of the Taguchi L9 array, has low gas penetration and no fingering effect. In part 7.1, which was produced with the settings specified by the 7th row of the Taguchi L9 array, it can be observed that the gas advances beyond the gas channel and pushes into the wall of the part.

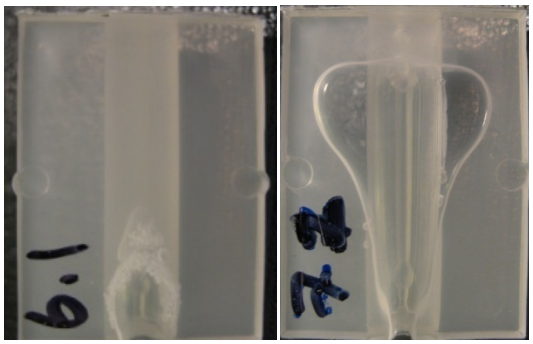

Figure 4-4: Fingering Width on Polypropylene Experimental Part

Gas fingering into the walls is not desirable because it weakens them. Also, when fingering occurs, gas may sometimes form a bubble and get trapped in the thin-wall sections of the part where it is unable to vent fully [44]. Figure 4-5 presents one part made with the settings specified by each of the rows in the Taguchi L9 array. The parts

made with the settings specified by the row numbers 1, 4 and 7 had larger amounts of gas fingering into the walls; these parts were all made with low level of *shot size*.

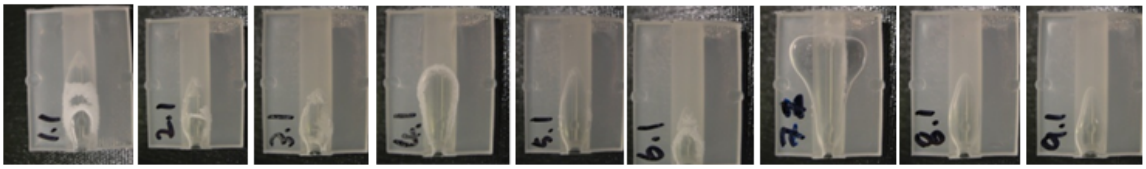

Figure 4-5: Polypropylene Experiment parts

4. 1.2 Simulation Results for Polypropylene

Figure 4-6 shows the results of the Moldflow® simulation for parts made with the settings specified by each of the row numbers in the Taguchi L9 array. The colored region is hollow and represents the penetration of the nitrogen gas in the parts.

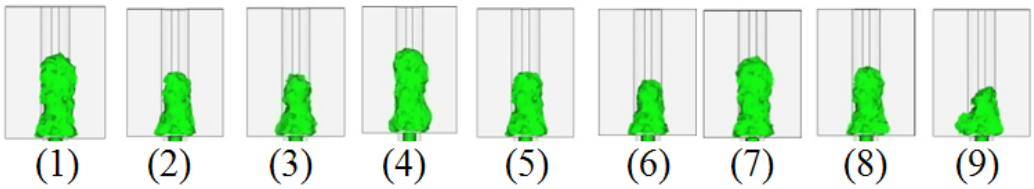

Figure 4-6: Moldflow® Simulation Polypropylene Trial 1-9 from left to right

The results of the Moldflow® simulation predicted the gas penetration very well. Part numbered 1, 4 and 7 had the highest gas penetration in both the experiment and the simulation. However, the fingering effect patterns predicted by the Moldflow® simulation were very different from the experiment as can be seen by comparing Figure 4-7 with Figure 4-8.

Table 4-3: Rank Significance of Processing Variables for Simulation with Polypropylene

	Melt Temperature	Shot Size	Gas Pressure	Gas Delay
Gas Penetration	3	1	2	4
	17.3%	62.0%	18.7%	2.0%
Fingering Effect	2	1	4	3
	35.0%	35.1%	8.9%	21.0%

Table 4-3 shows the rank and the per cent significance of each of the processing variables based on the calculated S/N ratios. The simulation predicts effect of the processing variables on the *gas penetration length* extremely well. In the case of the *fingering width*, the simulation overestimates the effect of the *shot size*, and underestimates the effect of the *gas pressure.* The discrepancy between Figure 4-7 and Figure 4-8 may be a result of this difference.

Figure 4-7 shows the pictures of polypropylene parts with the processing conditions according to the 4th row of the Taguchi L9 array from the simulation and from the experiment. Comparing simulation with the experiment there are some differences in the flow of material. Polypropylene permits the gas to flow in a manner that the widest bubble is on top of the cavity. On the other hand, the simulation looks different and it shows the widest area is at the gate where gas is introduced into the cavity.

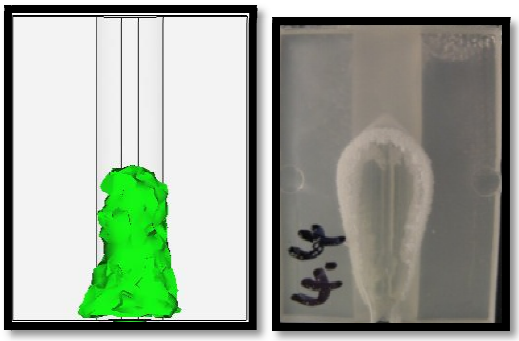

Figure 4-7: Polypropylene Simulation vs. Experiment Array number 4

Figure 4-8 shows the pictures of polypropylene parts with the processing conditions according to the 7th row of the Taguchi L9 array from the simulation and from the experiment. In this case the simulation underestimated the fingering effect away from the gate and overestimated the fingering effect near the gate.

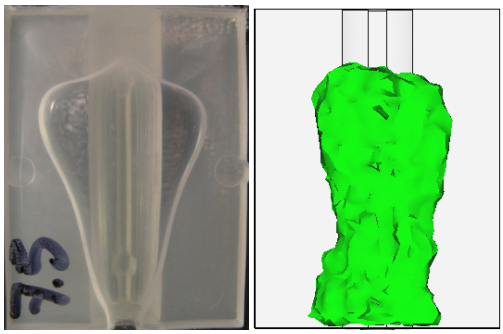

Figure 4-8: Polypropylene Simulation vs. Experiment Array number 7

The temperature pattern matches the shape of the gas bubble in the part in Figure 4-8. The gas bubble occupies the regions of higher temperature. This corresponds to the regions of molten material which can be displaced as the gas penetrates the part as shown in Figure 4-18(1).

4.2 Results for SUSL316L Feedstock

The results of the experiment with the SUS316 feedstock are presented here. This is followed by the results of the computer simulation and a comparison of the results from two approaches.

4.2.1Experiment with SUSL316L Feedstock

Figure 4-9 shows the main effect plot for *gas penetration length* and Figure 4-10 the *fingering length* in the *SUS316L feedstock* experiment. The pattern of effects of the

variables is quite different from the processing of polypropylene. All the processing variables appear to have significant effects on both gas penetration and on fingering. The *gas penetration length* is large when the *melt temperature* is high, but reduces when it is medium. The *fingering width* is large when the *melt temperature* is high, and small at the medium and low settings. The *gas penetration length* is large when the *shot size* is low, and it is small when the *shot size* is medium. The *fingering width* is large when the *shot size* is low, and it is small when the *shot size* is high. Both *gas penetration length* and *fingering width* are large when the *gas pressure* is medium, and both are small otherwise. Both *gas penetration length* and *fingering width* are large when the *gas delay time* is low, and both are small when the *gas delay time* is high.

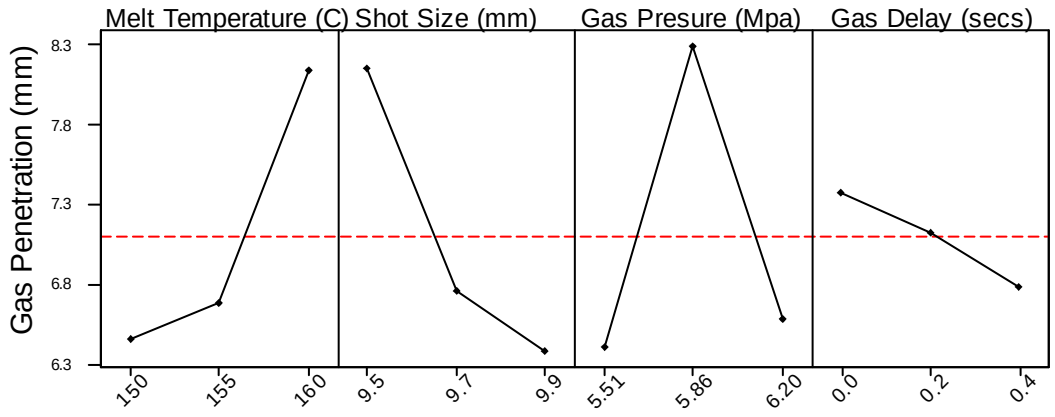

Figure 4-9: Main Effect Plot Gas Penetration Length SUS316L Experiment

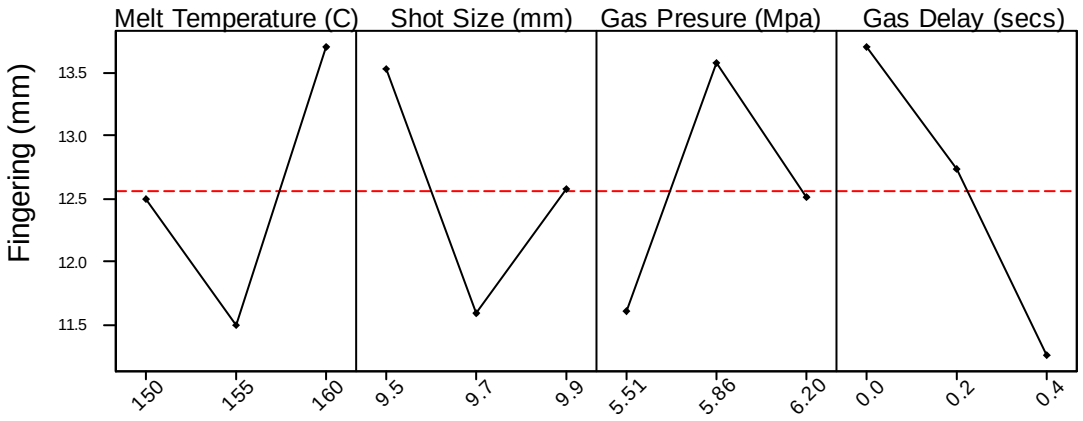

Figure 4-10: Main Effect Plot Fingering Width SUS316L Experiment

The average of five samples for the *gas penetration length* and the *fingering width* are shown for each row in the Taguchi orthogonal L9 array for *polypropylene* in Figure 4-11. The behavior of the *SUS316L* feedstock is dramatically different from the behavior of *polypropylene* when Figure 4-11 is compared to Figure 4-3. The *gas penetration length* for the powder metal feedstock is less than the *fingering width*. This behavior is exactly the reverse of the behavior of polypropylene. The explanation for this is provided in Section 4.4.

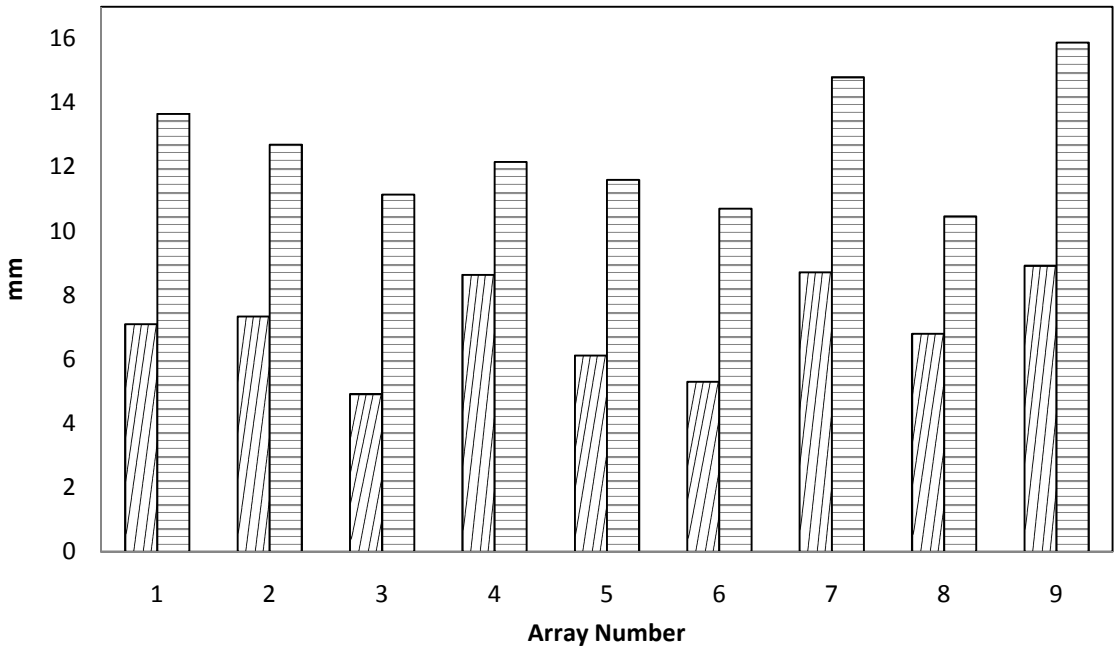

Figure 4-11: Experimental Gas Penetration vs. Fingering Width for SUS316L

The signal to noise ratio (S/N ratio) for maximum *gas penetration length* and signal to noise ratio for minimum *fingering width* of the processing variables was calculated. Table 4-4 shows the rank and percent significance of each of the processing variables based on the calculated S/N ratios.

Table 4-4: Rank Significance of Processing Variables for Experiment with SUS316L

	Melt Temperature	Shot Size	Gas Pressure	Gas Delay
Gas Penetration	3 27.4%	1 31.5%	2 30.0%	4 11.1%
Fingering Width	4 23.3%	1 28.7%	3 23.6%	2 24.4%

All four variables have equally significant effect on the *fingering width*. *Gas pressure, shot size* and *melt temperature* were the variables that affect *gas penetration length* with higher significance; the difference in percentages is very small, therefore all three of them

could be considered as the main effect variables. The gas delay has only a small effect on the *gas penetration length*.

This difference between the effect of *gas delay* on SUS316L and the polymer could be related to the fast cooling of the powder metal. When the powder metal feedstock is injected it freezes very fast due to its high thermal conductivity and low melt temperature and this stops the gas from penetrating further; therefore if the *gas delay* is high, the chance of penetrating through the gas channel is small, resulting in small *gas penetration length*, and instead the gas flows into the nominal walls of the part.

From the main effect plot for SUS316L in Figure 4-11 and Figure 4-12 the optimal parameters for a maximum *gas penetration length* and the variables for the minimum *fingering width* are shown in Table 4-5.

Table 4-5: Optimum variables for Gas Penetration and Fingering Width in SUS316L Experiment

Variables	Maximum Gas Penetration	Minimum Fingering
Melt Temperature	High	Low
Shot Size	Low	High
Gas Pressure	Medium	Medium
Gas Delay	Low	High

Figure 4-12 presents one part made with the settings specified by each of the rows in the Taguchi L9 array. It was necessary to break open the parts to be able to measure the gas penetration and the fingering effect in each of the parts made. The exposed areas are the regions of *gas penetration length* and *fingering width.*

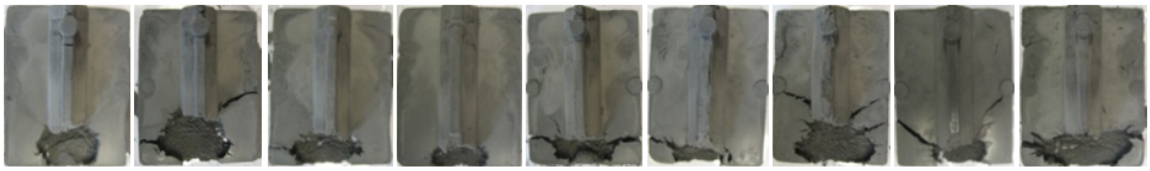

Figure 4-12: SUS316L Experimental parts, Parts were open to measure the *gas penetration length* and *fingering width*

4.2.2 SUSL316L Simulation Results

Figure 4-13 shows the results of the Moldflow® simulation for parts made with the settings specified by each of the row numbers in the Taguchi L9 array. The colored region is hollow and represents the penetration of the nitrogen gas in the parts.

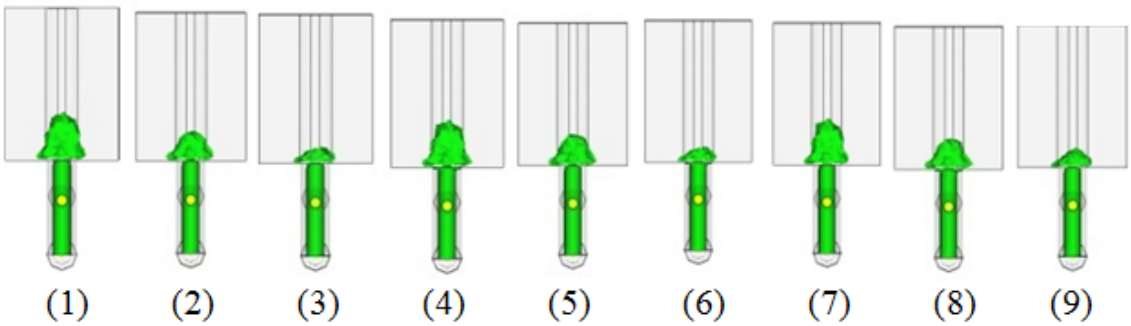

Figure 4-13: MoldFlow® Simulation for SUS316L. Trial 1-9 from left to right

MoldFlow® failed to predict the gas penetration behavior correctly in SUS316L. As shown in Figure 4-13, the gas penetration and fingering were generally higher than what the simulation estimated.

Table 4-6: Rank Significance of Processing Variables for Simulation with SUS316L

	Melt Temperature	Shot Size	Gas Pressure	Gas Delay
Gas Penetration Length	3 14.4%	1 64.9%	2 18.6%	4 2.1%
Fingering Width	4 3.6%	1 72.6%	3 3.6	2 16.1%

A comparison between Table 4-6 and Table 4-4 shows that the simulation and experimental significance estimates are very different. For gas penetration, Moldflow® estimated the *shot size* to have 64.9% of the effect, compared to 31.5% from the experiment. Therefore, Moldflow® overestimated the significance of the *shot size* and underestimated the significance of the other variables. In the case of fingering, Moldflow® again overestimated the effect of *shot size*, and underestimated the effect of *gas pressure*; however, Moldflow®'s estimate of the effect of melt temperature and gas delay agree with the experiment results. Moldflow failed to take account changes in material properties.

Before the gas assisted injection molding parts were made, it was necessary to run short shot experiments. Four short shots with increasing material volume are shown in Figure 4-14. It is possible to observe the jetting effect in these short shots of powder metal injection. As can be seen in Figure 4-14, the metal jets rapidly to the end of the channel before it starts filling the rest of the cavity. This observation helps understand the way gas will flow, because metal freezes very fast; therefore, when nitrogen is being injected there is not a lot of time for it to go through. The jetting effect can occur when gating into a thick, open cavity. The melt tends to flow into a deep cavity, rather than develop as a fountain flow front. When jetting occurs, the molded part will have a poor surface appearance, and a rope-like jet shape; also, the material injected cools during the early stages of the mold filling process and does not weld together properly [41].

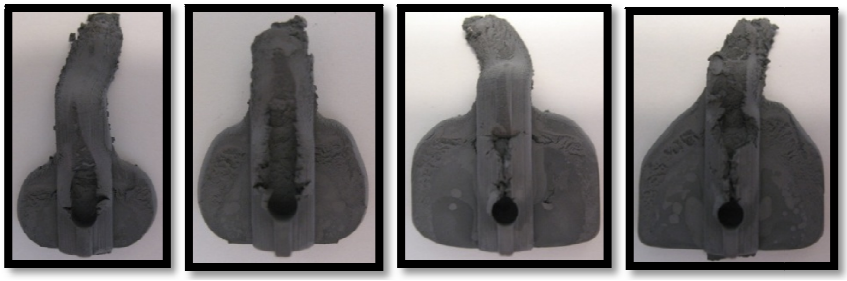

Figure 4-14: Short Shot Behavior of PIM with Different Shot Size

The short shots for the polypropylene material showed a different behavior from the short shots of SUS316L. The differences between the materials can be compared by looking at the pictures in Figure 4-14 and Figure 4-15. There was no jetting effect visible in the polypropylene, but significant sink marks were present.

Figure 4-15: Short Shot Behavior of Polypropylene with Different Shot Size

Figure 4-16 shows a complete part before measurements of *gas penetration length* and *fingering width* were done. The powder metal parts appear to have a clear and smooth surface showing clear detail of the shape of the part.

Figure 4- 16: SUS316L Parts before Measuring *Gas Penetration Length* and *Fingering Width*

Figure 4-17 illustrates the way one of parts looks like after setting up the experiment with the optimal conditions to get the maximum gas penetration. Observe that the gas penetrated more into the gas channel in the optimum case compared to the trial parts made in the experiment shown in Figure 4-12.

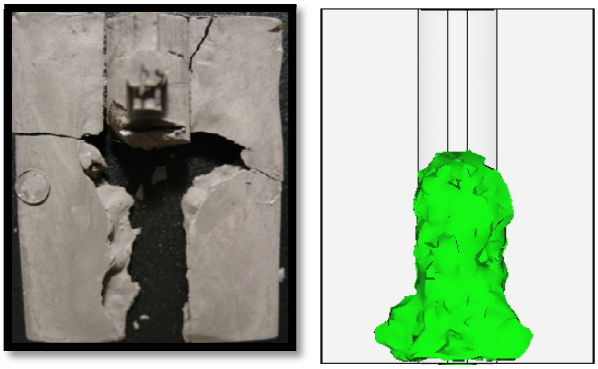

Figure 4- 17: Optimal Shot SUS316L with simulated shot

Figure 4-18 shows the bulk temperature profile of the part that was generated by MoldFlow®. In both cases, the hottest region is in the channel, and this is why the gas tends to follow the channel. The poor thermal conductivity of the polypropylene allows a high temperature gradient at the skin, and this allows the gas to flow easily through the core. For polypropylene, here is a 24.3 ºC difference between the highest temperatures which occurs in the channel compared to the lowest temperature which occurs on the wall; but for SUS316L, this difference is only 4.9 ºC. Thus, for SUS316L, the temperature gradient is small and the material freezes all over very fast.

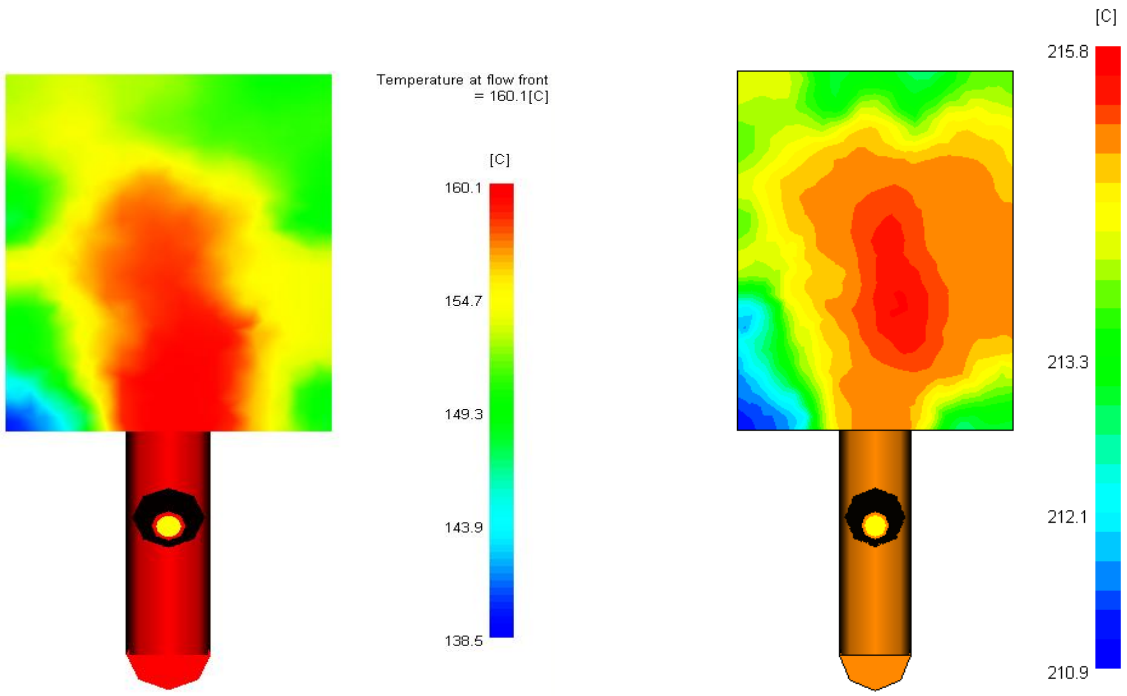

(1) Polypropylene (2) SUS316L

Figure 4-18: Thermal Analysis, center of Polypropylene part remains hotter in gas channel than SUS316L

It is also possible to observe the temperature gradient across the cross-section in Figure 4-19. For the polypropylene material, the interior is maintained much hotter than the surface and so allows better gas penetration. For SUS316L, the low thermal gradient allows the whole region to freeze fast. In fact, the fingering patterns are very similar to cross-section temperature profiles. This indicates that, the temperature after filling the cavity is more critical to fingering than other factors; however, this is not a conclusive finding.

(1) Polypropylene (2) SUS316L

Figure 4-19: Cross sectional area showing temperature analysis of both materials

4.4 Analysis of Residual Wall Thickness (RWT)

Once the optimal value was established for this experiment, the residual wall thickness of the parts (RWT) was observed. Each of the parts was analyzed through the cross-sectional area of the part by measuring the bottom, left and right sides of the gas channel. Figure 4-20 shows the location of the measurements. With the analysis of RWT it was found that the wall thickness was not uniform in the parts, especially in the beginning of the part, where gas is injected. The residual wall thickness in upper curved sections was thicker the region near the bottom.

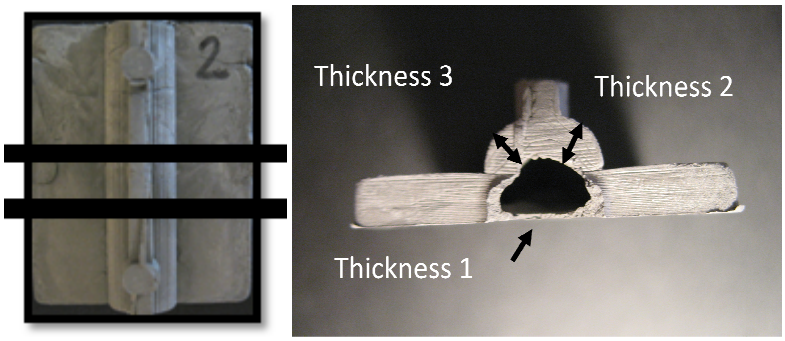

Figure 4-20: Measurement Region of parts RWT

Figure 4-21 shows the wall thickness at the cross-section near the gates. The wall thickness at the bottom surface is small. In addition, the regions in the wall where

fingering was observed also had small thickness on the top surface. These thin regions are critical and so would result in poor part strength.

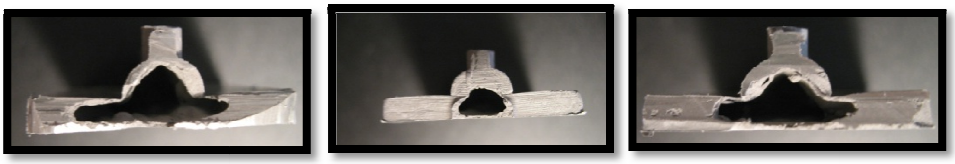

Figure 4-21: Parts without uniform wall thickness

An empirical formula from Findeisen et al research [47] is used to compare the residual wall thickness results from the polypropylene material.

$$s = r/3 \qquad \text{Eq. 4.1}$$

where:

s = skin thickness (same as residual wall thickness)

r = radius

The radius of the gas channel used in the cavity is 3.5 mm. From above equation, estimated RWT is 1.17 mm. And measured wall thickness at various location and percent deviation from calculated RWT are shown in Table 4-9.

Table 4-7: Residual Wall Thickness Measurements for Polypropylene Material

	Thickness1 (mm)	Thickness2 (mm)	Thickness3 (mm)
1	0.26	3.43	3.25
2	0.32	3.31	3.17
3	0.35	3.38	3.14
4	0.34	3.21	3.11
5	0.32	3.50	3.07

From Table 4-7, Thickness 1 which is the bottom section of the cavity showed only 22 to 29% of the estimated RWT. However, for the Thickness 2 and 3 showed about 178% higher than estimated RWT. This difference mainly comes from material availability and gate location. Further research needs to be done to evaluate RWT versus gas entrance point. Published literature indicates that the uniformity of *residual wall thickness* in fluid assisted *injection* molded parts could be improved by adopting differential mold temperatures [46].

CHAPTER V

CONLUSIONS

The Taguchi analysis was used to reduce the number of experiment trials and to find the optimum processing conditions that give a maximum *gas penetration length* with minimum *fingering width*. The processing variables used for this experiment were *gas pressure, gas delay, melting temperature,* and *shot size*. This process was simulated using MoldFlow software and compared with the experiment results.

The results showed that the *polypropylene* fills the mold uniformly as the flow front proceeds from the gate to the end of the cavity. On the other hand the powder metal feedstock *SUSL316L* fills the gas channel all the way to the end of the cavity and then starts filling the rest of the mold; further, the high thermal conductivity leads to fast cooling and these effects result in poorer gas penetration.

Results from simulation and experiment were graphed in main effect plot and ranked on S/N ratio tables. *Polypropylene* experiment results showed that *shot size* had the highest significance among all the variables for both *gas penetration length,* with a portion of 41.0% of the effect, and also for *fingering width,* with 59.3% of the effect. For *gas penetration length,* the *gas pressure* was ranked second with 24.4% of the effect, followed by *melt temperature* with 19.2% of the effect, and the *gas delay time* was the

least important parameter with 15.2% of the effect. In the case of the *fingering width* the main variable affecting is shot size with almost 60% of significance, followed by the next three variables *melt temperature*, *gas delay time* and *gas pressure* were almost equally significant. The simulation predicts effect of the processing variables on the *gas penetration length* extremely well. In the case of the *fingering width*, the simulation overestimates the effect of the *shot size*, and underestimates the effect of the *gas pressure.*

For SUS316L results in experiment and simulation all four variables have equally significant effect on the *fingering width*. *Gas pressure, shot size* and *melt temperature* were the variables that affect *gas penetration length* with higher significance; the difference in percentages is very small, therefore all three of them could be considered as the main effect variables. The gas delay has only a small effect on the *gas penetration length*.

A part was fabricated with the optimal processing conditions identified by the Taguchi analysis and it was found to have the largest *gas penetration length* and consequently the lowest material consumption. With the highest *gas penetration length* the part also showed to have a maximum *fingering width.* The simulation and experimental results were similar; but the simulation of both materials failed to predict that the powder metal feedstock would fill the gas channel first.

Residual wall thickness measurements showed that parts injected with gas do not have a uniform wall thickness. Each of the parts was analyzed throughout the cross-sectional area of the part by measuring bottom (thickness 1), right (thickness 2) and left (thickness 3) sides of the part. Thickness 1 which is the bottom section of the cavity showed only 22

to 29% of the estimated RWT. However, for the Thickness 2 and 3 showed about 178% higher than estimated RWT. This difference mainly comes from material availability and gate location. Further research is needed to evaluate RWT away from the gas entrance point.

REFERENCES

[1] Douglas M. Bryce, Plastic injection molding: mold design and construction fundamentals, Society of Manufacturing Engineers; 1 edition, 1999, page 1-3

[2] Robert A. Malloy, Plastic part design for injection molding: an introduction, Hanser Gardner Publications Inc., 1994, page 64

[3] Edward A. Muccio, Plastics processing technology, ASM International, 1994, page 151

[4] Gerd Pötsch, Walter Michaeli, Injection molding: an introduction, 2008, page 4

[5] Edward A. Muccio, Plastic part technology, ASM International, 1991, pages 64-69

[6] Tim A. Osswald, Lih-Sheng Turng, Paul J. Gramann, Injection Molding Handbook, Hanser Gardner Publications, 2007, page 395

[7] Cleveland Brad, Prototyping Process Overview, Advanced Materials & Processes, volume 7 July 2009

[8] Chee Kai Chua, Kah Fai Leong, Chu Sing Lim, Rapid prototyping: principles and applications, World Scientific Publishing Co. Pte. Ltd, 2003, Pages 35-42, 214-217

[9] R.V. Nambiar, K.H. Lee, D. Nagarajan, “Stereolithography mold life extension using gas-assisted injection”, Rapid Prototyping Journal, 13/2 (2007) pages 92–98

[10] Todd Grimm, User's guide to rapid prototyping, The society of Manufacture Engineers, 2004, page 79

[11] G.J. Shu, K.S. Hwang, Y.T. Pan, Improvements in sintered density and dimensional stability of powder injection-molded 316L compacts by adjusting the alloying compositions , Acta Materialia March 2006 (Vol. 54, Issue 5, Pages 1335-1342)

[12] J. Avery, Gas-Assist Injection Molding: Principleons and Applications, Hanser Gardner Publication Inc., Cincinnati, 2001.

[13] Seong-Yeol Han, Jin-Kwan Kwag, Cheol-Ju Kim, Tae-Won Park, Yeong-Deug Jeong, A new process of gas-assisted injection molding for faster cooling, Journal of Materials Processing Technology Volumes 155-156, 30 November 2004, Pages 1201-1206 Proceedings of the International Conference on Advances in Materials and Processing Technologies: Part 2

[14] Hansen, Michael. “Application Examples for Gas-Assisted Injection Molded Parts,” in Proceedings of the SPE Structural Plastics Division Conference. Boston: Society of Plastics Engineers, 1999.

[15] Hansen, Michael. “Processing Basics for the Design of Gas-Assisted Injection Molded Parts,” PhD thesis. Aachen, Germany: Shaker Publishers, 1996.

[16] Chen S.C. , Dong J.G., Mechanical Engineering, Chung Yuan University, Jeng M. C. Mechanical Engineering, National Central University, Yeh C.H, Yulon Motor, Ldt Taiwan, Case Study “The Application of Gas-Assisted Injection Molding to Automotive Parts”, Paper No 17-01

[17] Bryce, Douglas M, “Plastic injection molding: material selection and product design fundamentals”, 1997, pages 2-3.

[18] De Hoyos, Manuel, Gas-Assisted injection molding: A study on the effect of processing variables on bubble formation, 2009, page 4

[19] Clark, Christopher L, “Overcoming process control challenges of Gas-Assist Injection Molding” , ANTEC 1995, page 540

[20] Haagh, G.A.A.V., Peters, G.W.M., Van De Vosse, F.N. Meijer, H.E.H (2001). A 3-D Finite Element Model for Gas-Assited Injection Molding; Simulations and Experiments. Polymer Engineering and Science. 41(30, 449-465

[21] Bernie Miller, ANTEC REPORT, “Closed-loop controller aids gas-assist control”, Technology News, Plastics World July 1995.

[22] Gal Sherbelis, SPE, ANTEC 1995, Page 747

[23] Autodesk Moldflow Insight, November 2009, http://www.moldflow.com/stp/english/products/autodesk_moldflow_insight.php

[24] Moritzer E., Potente H., Theoretical and practical results for the gas injection molding process variant: Melt displacement into an overflow cavity. University of Paderborn, Polymer Department, D-33098 Paderborn, Germany, ANTEC1996 page 674-678.

[25] Fairbrother, F. and Stubbs, A. E., J. Chem. Soc., 1, 1935, pages 68-73

[26] Taylor, G.I., J. Fluid Mech.,10 m1961, pages 161-165

[27] Cox,B.G., J. Fluid Mech., 14 1962, pages 81-96

[28] Polinski, A.J. and Strokes, V.K. ANTEC proceedings, 39, 1993 pages 68-73

[29] Koelling Kurt W., "Gas assisted injection molding: Influence of processing conditions and material properties", Dept of chemical engineering. ANTEC 1996, pages 644-646

[30] Chen S.C., Hsu K.S., Chen N. T., Jong W.R., "Characteristics of gas penetration in gas-assisted injection molding", Department of mechanical engineering, Chung Yuan University, Chung-li, Taiwan 32023, R.O.C. Paper No- 15-01

[31] Chen Yew-Renn, Chen Tay-Yuan, Scientific Approach of Mold Design in Gas-Assisted Injection Molding: Sizing of Gas Channels, Materials Research laboratories, ITRI, Chutung, Hsinchu 310 Taiwan, Paper No. 14-02

[32] Huamin Zhou, Dequn Li, "Integrated simulation of the injection molding process with Stereolithography molds", International Journal of Advance Manufacturing and Technology, April 2005

[33] James G. Hemrick, Thomas L. Starr, David W. Rosen, "Release behavior for powder injection molding in Stereolithography molds", Rapid Prototyping Journal, Volume 7 . Number 2. 2001. pages 115-121

[34] S. Ahn, S. T. Chung, S. V. Atre, S. J. Park, R. M. German, "Integrated filling, packing and cooling CAE analysis of powder injection moulding parts", Institute of Materials, Minerals and Mining, November 2007

[35] B. Berginc, Z. Kampus, B. Sustarsic, "Influence of feedstock characteristics and process parameters on properties of MIM parts made of 316L", Institute of Materials, Minerals and Mining, November 2006

[36] M. Khakbiz, A. Simchi, R. Bagheri, "Investigation of rheological behaviour of 316L stainless steel–3 wt-%TiC powder injection moulding feedstock", Institute of Materials, Minerals and Mining, 2005

[37] http://www.plasticsnet.com/product.mvc/BOY-30-0001

[38] D.B. Ramalingam, "Extension of Stereolithography Mold Life Using Gas-Assisted Injection Molding", 2005, M.S. Thesis, University of Texas Pan American, Edinburg, TX.

[39] G.S. Peace, Taguchi Methods; A Hands- On Approach, 1993, Addison-Wesley,

://www.protocam.com/html/sls.html>

[44] Lin, Kun-Yeh, Chang, Fu-An, Liu, Shih-Jung, Using differential mold temperatures to improve the residual wall thickness uniformity around curved sections of fluid assisted injection molded tubes", International Communications in New York, NY

[40] Parvez M. A., Ong N. S., Lam Y. C., Tor S. B., "Gas-assisted injection molding: the effects of process variables and gas channel geometry", Journal of Materials Processing Technology, Volume 121, Issue 1, 14 February 2002, pages 27-35

[41] Robert A. Malloy, "Plastic Part Design for Injection Molding", Cincinnati, Hanser Gardner Publications, 1994, Pages 44-45, 108-111

[42] Hague R. J. M., "The use of Stereolithography models as thermally expandable patterns in the investment casting process. PhD thesis, University of Nottingham, January 1997.

[43] ProtoCAM, "Selective Laser Sintering", November 2009, <httpHeat & Mass Transfer; May2009, Vol. 36 Issue 5, Pages 491-497

[45] Zhu Jie, Chen Joseph, 2004, "Tensile Strength and Optimization of Injection Molding Processing Parameters Using the Taguchi Method, December 12 2009, http://www.ijme.us/issues/spring2004/TensileStrengthOptimzation.htm

[46] eFunda," Highlights of Selective Laser Sintering" December 14 2009, http://www.efunda.com/processes/rapid_prototyping/sls.cfm

[47] Costumer part net, "Injection Molding", December 14 2009, http://www.custompartnet.com/wu/InjectionMolding

[48] Costumer part net "Stereolithography", December 14 2009 http://www.custompartnet.com/wu/stereolithography

[49] Ryall Chris, Wimpenny David, "Rapid Prototyping technology as used on the Bombe Rebuild Project', December 14 2009 http://www.jharper.demon.co.uk/rptc01.jpg

[50] Gain Technologies 2001, December 14 2009, http://www.gaintechnologies.com/

[51] 3D systems, December 14 2009, http://www.3dsystems.com/products/datafiles/datasheets-1007/SLA/DS-Viper_Pro_SLA_System_07.pdf

BIOGRAPHICAL SKETCH

Edna Orozco was born March 21st 1983 and her permanent mailing address is Isla de Bahia 290, Torreon Residencial, 27268, Torreon Coahuila, Mexico. She developed interest for the engineering field in high school. Therefore she started the degree of Industrial Engineering at the *Instituto Tecnologico de Monterrey, Mexico*. After studying for several semesters Edna decided to transfer to the University of Texas-Pan American. She finished the Bachelor of Science in Manufacturing Engineering and has been an active member in various organizations like the Society of Hispanic Engineers, the Society of Automotive Engineers, as well as the Society of Manufacturing Engineers. Edna Orozco had the opportunity to get certified on a Six Sigma Green Belt and Black Belt in the spring semester 2009. She was given an assistantship by the Manufacturing Department at the University of Texas-Pan American to pursue a master degree in Manufacturing Engineering. Throughout the master studies she researched and won the Best Graduate Student award in the College of Science and Engineering in the fall semester 2009. Working with students and combining this experience with research she decided to possibly heading for a PhD. Degree in Industrial Engineering.